NASA Technical Memorandum 108792

Evaluation of Visual Acuity with Gen III Night Vision Goggles

Arthur Bradley, Indiana University, School of Optometry, Indiana
Mary K. Kaiser, Ames Research Center, Moffett Field, California

January 1994

National Aeronautics and
Space Administration

Ames Research Center
Moffett Field, California 94035-1000

Table of Contents

Page

List of Tables and Figures v

Summary 1

Background 1

Simulating Nocturnal Environments 1

Previous Attempts to Measure NVG Performance 2

Problems with Previous Approaches. 2

Laboratory Simulation 3

Simulation Procedures 3

Measuring Visual Performance 4

Experimental Methods 5

Apparatus 5

Macintosh-Based Letter Acuity System 5

Viewing Set-Up 5

Experimental Procedure 5

Experimental Results 6

Unaided Vision Acuity Data 6

Foveal Acuity 6

Peripheral Acuity 6

Intensified Vision Acuity Data 6

Comparison of Unaided and Intensified Vision 6

Discussion 7

References 8

Tables and Figures 10

List of Tables and Figures

Tables

Table 1. Luminances, radiances, and Nvis radiances available during experiment

Table 2. Representative values of visible radiance (luminance) and Nvis radiance for several "standard" night sky condition

Figures

Figure 1. Plot of relative spectral sensitivities of human eye under photopic conditions (open squares) and spectral response of ITT Gen III image intensifier tube (filled squares).

Figure 2. Radiance spectrum for P4 phosphor display (Macintosh Gray-scale monitor).

Figure 3. Schematic representation of the calculation of luminance and NVIS radiance of our display monitor.

Figure 4. Reflection spectra of five commonly encountered materials plotted as percentage of incident radiation reflected at each wavelength.

Figure 5. Earth surface irradiance spectra for a variety of night illumination conditions.

Figure 6. Sample psychometric functions obtained with unaided vision both centrally and peripherally.

Figure 7. Same as figure 6 except with NVG vision.

Figure 8. Example of curve fitting procedure used to estimate VA (expressed as the log of monocular angular resolution (MAR) by interpolation).

Figure 9. Unaided VA as function of target luminance for two subjects (AB and TG).

Figure 10. Comparison of high-contrast unaided VA data from this study (open symbols) with those measured in earlier studies.

Figure 11. Monocular (filled symbols) and binocular (open symbols) unaided acuities for two subjects at three letter contrasts.

Figure 12. Unaided high (99%) contrast VA as function of target luminance for two subjects.

Figure 13. Unaided medium (40%) contrast VA as function of target luminance for two subjects.

Figure 14. Unaided low (10%) contrast VA as function of target luminance for two subjects.

Figure 15. VA as function of target eccentricity for a range of target luminances.

Figure 16. NVG-aided VA as function of target radiance (NVIS radiance) for two subjects (AB and TG).

Figure 17. Monocular (filled symbols) and binocular (open symbols) NVG-aided acuities for two subjects at three letter contrasts.

Figure 18. Unaided high (99%) contrast NVG-aided VA as function of target luminance for two subjects.

Figure 19. Unaided medium (40%) contrast NVG-aided VA as function of target luminance for two subjects.

Figure 20. Unaided low (10%) contrast NVG-aided VA as function of target luminance for two subjects.

Figure 21. The relationship between the lighting levels used in the laboratory experiment and those experienced in the nocturnal environment are shown.

Figure 22. The method for interpolating visual acuity expected under a variety of environmental conditions.

Figure 23. VA for aided (circles) and unaided (squares), for two reflectors (open = white paper, filled = green foliage) and for three different target contrasts: foveal.

Figure 24. Same as figure 23 except for 5° eccentric.

Figure 25. Same as figure 23 except for 10° eccentric.

Figure 26. Same as figure 23 except for 20° eccentric and for high (99%) target contrast only.

Figure 27. Visual acuity on a linear scale as function of target eccentricity for range of environmental conditions.

Figure 28. Visual acuity on a log scale as function of target eccentricity for a range of environmental conditions.

Evaluation of Visual Acuity with Gen III Night Vision Goggles

ARTHUR BRADLEY* AND MARY K. KAISER

Ames Research Center

Summary

Using laboratory simulations, visual performance was measured at luminance and night vision imaging system (NVIS) radiance levels typically encountered in the natural nocturnal environment. Comparisons were made between visual performance with unaided vision and that observed with subjects using image intensification. An Amplified Night Vision Imaging System (ANVIS6) binocular image intensifier, manufactured by ITT (employing their Gen III tube), was used. Light levels available in the experiments (using video display technology and filters) were matched to those of reflecting objects illuminated by representative night-sky conditions (e.g., full moon, starlight). Results show that as expected, the precipitous decline in foveal acuity experienced with decreasing mesopic luminance levels is effectively shifted to much lower light levels by use of an image intensification system. The benefits of intensification are most pronounced foveally, but still observable at 20° eccentricity. Binocularity provides a small improvement in visual acuity under both intensified and unintensified conditions.

Background

Two general issues are addressed in this investigation: (1) the very practical issue of establishing a feasible experimental model for predicting visual capability of Night Vision Goggle (NVG) users under nocturnal viewing conditions encountered in the real world, and (2) careful measurement of visual performance under low light levels with and without image intensification. Central to both of these issues are the requirements that NVGs operate over a wide range of night illumination levels and that NVG users be able to inspect targets with a wide variety of reflection spectra.

Simulating Nocturnal Environments

Simulating nocturnal environments in the laboratory would seem to be an easy task: By careful use of easily obtainable neutral density filters, the effective luminance of any laboratory target can be reduced to that of any target as seen under any level of night sky illumination. This approach has been used extensively in the previous NVG studies.

Although this straight forward solution to the problem of simulating the nocturnal environment seems simple enough, there are several complicating factors. First, the quality (accuracy and validity) of experimental measures of the nocturnal environment becomes an important factor. Second, because the source of surface illumination varies for different night sky conditions (e.g., moonlight compared with starlight), both the intensity and the spectral distribution of the surface irradiance will vary. This variation becomes even more significant because the reflectances of targets vary considerably across the spectrum. For example, green leaves reflect significantly more in the near infrared (IR) than does equally bright concrete. Third, the spectral response of the NVG is very different from that of the unaided eye. Therefore, any comparison between these two viewing conditions (i.e., NVG and unaided vision) made in the laboratory must match the radiance within these two different spectral ranges to those observed in the natural environment.

Fourth, although neutral density (ND) filters are generally considered to be spectrally neutral (spectrally flat density functions), many are only "neutral" within the visible range of the spectrum and only approximately so even within this range. Therefore a 3.0 ND filter used for a vision experiment may only be a 2.0 ND filter in the near infrared (the NVG spectral range). Finally, instrumentation typically employed in vision laboratories provides photometric data; that is, radiance that has been weighted by the human spectral sensitivity function (V_l) and integrated across wavelengths. Such measurements have very little significance for assessing the stimulus strength for an NVG user.

We set out to solve all of the above environmental simulation problems, and to develop an accurate and easily reproducible experimental model of nocturnally viewed targets suitable for comparing unaided (natural) night vision with aided (NVG) night vision.

*Indiana University, School of Optometry, Indiana.

Previous Attempts to Measure NVG Performance

Several published laboratory studies have examined the visual capabilities of observers using image intensifiers, some with Gen II image tubes and some with Gen III tubes. A number of studies have measured visual resolution using either visual acuity (VA) or contrast sensitivity (CS) tasks (refs. 1–6). The results from references 1–6 show some very clear generalities. First, VA seems to be improved over a range of mesopic and scotopic light levels when using image intensification (refs. 1, 2, 4, and 7). However, there are some inconsistencies in the data. For example, Hoover (ref. 1), using Gen II tubes, found a large improvement in VA even at luminance levels equivalent to that of the full moon. But Wiley et al. (ref. 2) and Wiley and Bradley (ref. 5) report that it is at about the same luminance level (full moon) that aided vision begins to lose its superiority over unaided vision. That is, at full-moon luminance levels, VA is better without NVGs. Measures of CS with NVGs are less common. Wiley et al. measured subject CS at four light levels with a Gen II system, whereas Still et al. (ref. 8) measured CS with a Gen III system. Wiley et al. (ref. 2) using gratings, and Wilkinson and Bradley (ref. 5), using 20/200 letters, report maximum CSs of near 10. However, Wilkinson and Bradley, using a grating contrast sensitivity chart (VisTech), report CS near 100 for mid-frequency gratings. Still et al. also report very high (greater than 100) CSs with NVGs. The best VAs typically range near 10 cycles/deg for gratings (ref. 4), and near 20/40 for high contrast letters for both Gen II and Gen III systems (refs. 4–6).

There are few reproducible standards in these data. In particular, the range of environmental illumination levels over which vision with NVGs is superior to that of unaided vision is unclear. The maximum contrast sensitivity is quite varied. No systematic analysis of the benefits of Gen III over Gen II have been performed (although in ref. 6 VA was compared for both systems). However, as shown by Kotulak and Rash (ref. 6), several more recent studies of VA with Gen III tubes report similar acuity values for a variety of night illumination conditions.

The variance in these data could originate from a several sources. First, there may be significant variation in NVG performance from one goggle to the next (although none has been shown). Also, the simulated night illumination levels may have varied significantly, because little care was taken to ensure the accuracy and representativeness of the simulation. For example, several studies report (or imply) using Kodak gelatin filters, which have very different optical densities in the near IR (optical density at 950 nm is approximately only 45% of that at 700 nm). The ND specification of the Kodak filters probably reflects the average optical density over the visible range and not that over the NVG range. Wiley and Holly (ref. 9), then Hoover (ref. 1), Levine and Rash (ref. 3), Wilkinson and Bradley (ref. 5), and more recently Still et al. (ref. 8) all used Kodak Wratten filters to attenuate the signal. Filters that are only calibrated for the visible range (400-700 nm) often deviate significantly near the edges of this range, and can be substantially different in other spectral regions. For example, a 3.0 ND gelatin filter, such as that used by Still et al. probably has an optical density of 2.65 at 950 nm. Therefore, when comparing unaided and aided vision with these filters, an unfair advantage is given to the NVG in that it is effectively being tested at higher light levels. The converse can also occur. For example, many vision experiments employ standard vision charts with black paint or ink on a white background. These charts have maximum reflection in the visible range, whereas some targets in the natural environment have maximum reflectance in the near-IR (e.g., green foliage) and very attenuated reflectance in the visible range. Therefore, the visual improvement seen in the laboratory may significantly underestimate that attainable in the natural environment where unaided vision will be significantly reduced owing to the low reflectance of many of the targets in the visible spectrum.

Problems with Previous Approaches

Any attempt to simulate the night sky by providing a fixed illuminant (e.g., a filtered tungsten bulb) at a fixed voltage suffers in two respects. First, the simulation is only approximate (e.g., compare figs. 4 and 5 of ref. 6). Second, the spectrum of the night sky varies considerably with environmental changes (ref. 10). Third, it is insufficient to simulate only the illumination source; the spectral characteristics of the reflector must also be considered since the NVG user primarily views targets that are reflecting the night-sky illumination. Fourth, very few modern vision laboratories employ reflected targets for their studies of human visual performance. Such stimuli have been superseded by the more flexible and more easily controlled stimuli presented on video display terminals. Therefore, studies that simulate the nocturnal environment with projectors and light sources that illuminate reflecting targets necessarily preclude virtually all modern experimental methods and essentially relegate NVG research to pre-1960's methods.

The second problem above can be partially solved by employing several different filtered light sources, as is done with the night-sky projection device manufactured

by Hoffman Engineering Corp. and used by Kotulak and Rash (ref. 6). However, this solution to the second problem is only approximate and it does not solve problems one, three, and four.

Laboratory Simulation

We treat both the unaided nocturnal viewer and the NVG user as essentially "monochromatic" systems, which are distinct from the trichromacy observed in diurnal human vision and also available in many electro-optical systems. Therefore, unaided vision and NVG nocturnal vision behave as a single integrator of radiant flux, but each with a different spectral response function (fig. 1). In our calculations of effective radiance, we have used the Gen III spectral response curve to assess night vision imaging system (NVIS) radiance. For the human spectral sensitivity, we have the choice of the V_l (cone response) or V'_l (rod response) function. Most of the research presented in this project concerns primarily foveal and hence cone-based vision. However, most of the nocturnal environment does not provide photopic levels of illumination. For example, according to table 5.2 of Hood and Finkelstein (ref. 11), rod saturation occurs at considerably higher light levels than are available during the brightest of nights (full-moon illumination), and hence all night environments provide either mesopic or scotopic light levels. According to Hood and Finkelstein's table 5.2, most of the night environments can provide target luminances that exceed the cone absolute threshold, and therefore would be considered mesopic. Because no simple mesopic spectral sensitivity curve exists, we have chosen to use the V_l function. However, because of the spectral similarity of the V_l and V'_l, and the generally quite flat irradiance spectra (fig. 4, ref. 11) and reflection spectra (fig. 5, ref. 11), recomputing our luminance data using V'_l would produce fairly minor changes in the final conclusions.

There is also some uncertainty about the precise nature of the Gen III NVG spectral weighting function. Clearly, the image intensifier tube provides the most significant spectral characteristics, but these can be modified slightly by optical filters placed in front of this tube (e.g., blue-blocking filters).

Under nocturnal illumination conditions, these two systems (NVGs and unaided eye) produce a response that is determined by the amount of radiance within these two largely non-overlapping spectral bands. In order to simulate the night environment in our laboratory, we simply match the integral of the weighted spectral output of our computer-controlled video display to the integral of the weighted radiance spectrum for real targets illuminated by real night-sky illumination spectra. The video display spectrum is never altered, but the display intensity is controlled by use of calibrated neutral density filters. To achieve the same target intensity with the unaided eye will require different filters than when viewed through the NVG; the required filter density will also vary as a function of the targets' reflection spectra.

Simulation Procedures

The first task in this simulation procedure involved a spectral calibration of our laboratory display and of all filters to be used. This entailed blocking all wavelengths beyond the limit of our calibration equipment (830 nm), and performing an integration weighted by spectral sensitivity. The second task required an examination of the literature to determine spectral characteristics of night-sky illumination and object reflection spectra.

We employed a display with a P4 phosphor that was calibrated with a spectro-radiometer (fig. 2). Unfortunately, our spectral calibration only extended to 830 nm. Thus, we were unable to determine the radiometric output of the display beyond this wavelength. In order to eliminate the possibility that the display was producing any significant radiance above 830 nm which would be detected by the NVG, we employed an IR-blocking filter interposed between the NVG and the display (see fig. 3). This filter had high transmission below 700 nm, and virtually zero transmission above 770 nm. The filtered spectrum was altered little below 700 nm (fig. 3, panel 3). We then weighted our filtered display spectrum by the visual and the NVG spectral sensitivity curves (fig. 3, panel 4); the resultant luminance and NVIS radiance spectra can be seen in panel 5. There is very little NVIS radiance because of two factors. First, the IR blocking filter effectively eliminates all spectral energy beyond 770 nm, and second, the P4 phosphor is specifically designed to concentrate its energy within the visible spectrum. An expanded version of the NVIS radiance spectrum is shown in panel 6 of figure 3.

The second data set necessary to complete the simulation was more difficult to acquire. There are several sources that describe the reflection spectra of targets over the visible and near-IR range. We have utilized a source provided by Roy Holms of ITT, who is a senior engineer involved in NVG design and manufacture. He also provided us with a library of night-sky illumination spectra.

Sample reflection spectra are shown in figure 4. It is important to note the differential reflection for near-IR and the visible spectrum. For example, although

concrete reflects more than green foliage in the visible spectrum, the converse is true in the near-IR.

Determining the night sky illumination levels is a more complicated, for a number of reasons. First, the data are inherently more difficult to obtain because of the low signal strengths involved. For example, over a 10 nm spectral range there may only be a fraction of a pico Watt of radiant power incident per cm of the earth's surface. Second, there is the problem of determining which night sky is representative. Although the military employ standard night sky categories (e.g., full moon, 1/2 moon, starlight, cloudy starlight,), the night sky provides a continuously variable and multivariate illumination source. Cloud density, cloud height, atmospheric water content, proximity to city lights, moon azimuth and elevation, location of measurement site, time of year, etc. all affect the surface irradiation spectra (refs. 10, 12, and 13). Thus, the low signal strength may compromise the accuracy of any data set, and the variability of the night sky may affect the validity of any given standard.

Finally, there are different methods for measuring the night sky. For example, a directionally biased detector can be directed at a certain portion of the night sky. Alternately, an integrating sphere can measure surface irradiance without any directional bias. A third method uses a radiometer to measure the radiance of a surface target (with known reflectance) that is being irradiated by a large segment of the sky. This third method was employed by Vatsia et al. (ref. 10) and by Stefanik (ref. 13) in the two most complete studies, both carried out by the U.S. Army. This approach clearly has the most direct application for night vision in that it measured the spectra of a surface object. As long as the reflection spectrum is known, the irradiance spectrum can easily be determined by the following approximate equation:

$$\text{Irradiance } (W/m^2) = (\pi/\text{reflection coefficient}) \times \text{Radiance } [W/(sr \cdot m^2)]$$

where

m = meters
sr = steradians

It is important to realize that these data are often described as "night-sky radiances" (or radiant sterances); yet, as pointed out by Vatsia, et al., using reflection spectra from a surface may differ from direct measures of, for example, the moon (ref. 10). The data included in the RCA handbook (ref. 12) allow a more complete description because they provide surface irradiance for a variety of moon elevations and phases. The primary difference between the data employed in this study and those of Vatsia et al. is that their full moon condition was not truly full moon. Also, the mid-spectrum (550-600 nm) peak observed in night glow is smaller. The spectral data in figure 5 emphasize the intensity and spectral changes that occur with changing night sky conditions. The following representative night-sky conditions are used:

1. Full moon (FM) (100% moon, at 90° elevation)
2. Half moon (50%M) (50% moon, at 75° elevation)
3. 20% Moon (20%M) (20% moon, at 30° elevation)
4. Starlight (SL)
5. Cloudy starlight (CSL)

We determine the target radiances under a variety of night-sky conditions by a simple four-step calculation: (1) multiply the Irradiance values by the reflection coefficients at each wavelength, (2) multiply by pi, (3) weight the resulting spectra by either the NVG or the visual spectral sensitivity function, and (4) integrate across wavelength. These integrals can then be matched to those determined for our laboratory stimulus.

We can now assert that a given visual performance observed in the laboratory can be expected under known conditions in the natural environment. For example, we can calculate which laboratory conditions (i.e., which ND filters) will match the NVIS radiance and luminance expected for viewing a given target (e.g., concrete) under a given illumination condition (e.g., 20% moon). We can therefore predict the visual performance capability of NVG users under these conditions.

Measuring Visual Performance

Clearly, there are many skills that characterize human visual performance. However, determining the visual performance measures that will be most valuable as indicators of the end users' performance capabilities is very difficult. A few studies have tried to show how particular laboratory measured visual skills correlate to environmentally realistic performance skills. For example, investigations of this issue are reported in references 14–19. Disappointingly, conflicting results have been observed (e.g., compare the results of refs. 14 and 17).

In spite of the obvious criticism that very few operational scenarios require NVG users to read fine print, measures of visual acuity are still the standard visual metric employed in NVG studies. Although this may appear inconsistent with the visual requirements of the NVG user, it is worth considering the general philosophy behind such a trend.

Most of spatial vision can be considered low-pass or bandpass in nature. For a wide variety of tasks (depth perception from stereopsis, target resolution, contrast detection, position alignment, etc.) the visual system has a high-frequency limit beyond which the skill cannot be performed. Any decline in high-frequency sensitivity caused by additional low-pass filtering is therefore likely to affect many visual skills. In its simplest case, low-pass filtering that eliminates high frequencies from the retinal or neural image will preclude any perception arising from this frequency range in the stimulus. It is easy to measure such additional low-pass filtering by monitoring visual acuity, which will be affected by either optical, instrument, or neural filtering.

Most of the data presented in this report describe experiments to measure visual acuity. However, in order to examine visual performance over a wide range of contrasts, we have measured visual acuity for high-contrast (99%), medium-contrast (40%) and low-contrast (10%) letters. It is important to monitor thresholds for a wide range of spatial detail in order to assess the effect of NVGs on the detection and perceptual abilities for low-contrast targets, and for targets containing a wide range of spatial detail.

Of particular interest to this project is the effect of image intensification on visual performance across the visual field. These experiments have a direct implication for design strategies that consider display size. Previous studies of visual acuity as a function of target luminance show that the rapid decline in acuity seen foveally is virtually absent for peripheral targets (refs. 7, 20). That is, visual acuity for peripherally presented targets is virtually identical under scotopic and photopic conditions. If this is so, we might not expect to see the same advantage in peripheral vision that are provided for foveal vision by the NVG. Also, we have compared visual performance attainable monocularly with that reached binocularly. These data have some bearing on the issue of whether binocular, or biocular (i.e., the same image presented to both eyes), systems are expected to be superior to monocular image intensifiers.

Experimental Methods

Apparatus

All stimuli were displayed on a video monitor, and all test stimuli were controlled directly by computer.

Macintosh-Based Letter Acuity System

Letters were generated by a Macintosh II computer and were displayed on a high-resolution white monochrome monitor (P4 phosphor). All letters were darker than the white background. From a set of 10 letters (non-serifed letters where letter height and width were five times the bar width), the computer randomly selected single letters that were displayed on the center of the screen. Letter contrast (defined as $(L_S - L_l)/L_S$, where L_l = letter luminance and L_S = background screen luminance) ranged from 100% to 0.3%. The background luminance was set to maximum (120 cd/m^2). At the 10 ft viewing distance, the screen subtended 3.1° by 4.3° of visual angle. Letter size was varied from an equivalent of 20/400 to 20/10 (note acuities from 20/20 to 20/10 were measured with an increased viewing distance of 20 ft). Letter size could be varied in an approximate geometrical progression (equal log step sizes) between these two extremes. The letters had a uniform luminance, and each letter was presented in the center of the screen and remained on until the subject responded by identifying the letter.

Viewing Set-Up

Subjects viewed the monitor monocularly or binocularly in an otherwise unlit room. During monocular testing, one eye was occluded with an opaque occluder. Subject head positions were stabilized by using a chin rest. Spectrally calibrated neutral-density filters could be interposed between each eye or each entrance aperture of the NVG and the display. Light leakage was prevented by using light baffles and a specially engineered opaque tube, which fitted over the two NVG entrance apertures and carried circular ND and red-blocking filters.

Experimental Procedure

Subjects fixated on the center of the screen (foveal tests) or on a dim light displaced from the screen center (peripheral tests). Subjects were forced to identify each letter. Ten letters were presented (from a set of 12) at each letter size or contrast, and letter size/contrast was then reduced. This procedure was continued until subjects failed to identify at least three letters correctly. At this point testing was terminated and another filter condition was chosen.

A standard interleaved descending and ascending sequence of filters was employed. The sequence was reversed when a filter density was reached that prevented the subject from correctly identifying more than 50% of the largest or highest contrast letters. In effect we measured visual acuity or contrast sensitivity

over the largest range of luminance or NVIS radiance levels possible with our equipment. Two sample sets of raw data from a letter-acuity experiment are shown in figures 6 and 7.

Letter acuity was determined by fitting a Weibell function of the form

$$W(x - t) = 1 - (1 - g)\exp[-10^{b(x-t)}]$$

to the letter-acuity data, where g is chance performance (1/12 in these experiments); b is the slope of the psychometric function, and t the position of threshold. Threshold occurs when x = t, for W = 0.663. This function was fitted to the data using the software package Mathematica. An example of three fits is shown in figure 8. This approach estimates the letter size that would be expected to provide 66% correct letter identification.

Experimental Results

Unaided Vision Acuity Data

Foveal acuity– Monocular decimal VA is plotted in figure 9 for two subjects (AB and TG) as a function of display luminance. As expected, acuity falls off with decreasing luminance, but begins to asymptote at higher luminance levels. The asymptotic acuities for both subjects are close to 20/13. This acuity is considerable better than the 20/20 standard for "normal" vision, but not unusually high for near optimal viewing conditions (ref. 21). The circles show data for high-contrast letters; they are replotted in figure 10 with data from several earlier studies of the effects of luminance on VA (ref. 22–27). This comparison confirms that our methods for measuring VA produce results comparable to those in the earlier literature.

The effects of target contrast on VA can be readily observed in figure 9. Decimal acuity for 40% contrast letters is slightly lower (0.13 log units) than that observed for high-contrast letters. Acuities were degraded even further by reducing letter contrast to 10%. Maximum acuities barely exceeded 20/100, even at the highest luminances, and the range over which acuity was measurable was attenuated. At the lower luminances, contrast thresholds exceeded the stimulus contrast, and even the largest letters presentable in our experiment could not be resolved.

At each luminance level, and for each letter contrast we compared binocular VA with monocular acuities. Monocular acuities were obtained with each subject's dominant eye. The results (fig. 11) confirm earlier studies (e.g., ref. 28) in that a slight improvement is seen binocularly. Interestingly, for subject AB, this small improvement provided by binocular vision at photopic levels disappeared at the lowest luminances. There was also some indication of this trend in the data of subject TG.

Peripheral acuity– Unaided VA was measured over a wide range of luminances foveally and at 5°, 10°, and 20° eccentrically. These data are shown in figures 12–15. The familiar pattern is seen. For example, for high-contrast letters (fig. 12) the rapid decline in acuity with decreasing luminance, is restricted to the fovea, and at 20° (subject AB, diamonds) or 10° (triangles) the decrease in acuity from photopic to cone threshold is greatly reduced. Similar data have been reported previously (refs. 7, 20). This luminance independence of peripheral visual acuity is very significant. For example, if visual acuity at low light levels is the same as that at high light levels, the rationale behind image intensification as a vision aid is lost. The same trend was seen in the 40% contrast data (fig. 13), and the 10% contrast data (fig. 14). At 20°, the 40% and 10% letters became invisible because of the elevated contrast thresholds.

The trend showing that the superiority of foveal vision is restricted to photopic levels can be seen clearly in figure 15. Once target luminance has declined to <0.1 cd/m^2, acuity in the near periphery is equal to that in the fovea.

Intensified Vision Acuity Data

The same experiments that produced the data shown in figures 9–15 were then repeated with intensified vision. These data are plotted in NVIS radiance units (figs. 16–20), but the same trends observed in the unaided data can be seen here. For example, there is a decline in VA with decreasing NVIS radiance, and also with decreasing stimulus contrast (fig. 16). High-contrast acuity begins to asymptote at higher NVIS radiance levels.

The improvement in vision provided by a binocular view is less obvious with the NVG data (fig. 17). However, a small improvement in acuity is generally observed. VA declines with increasing eccentricity at high NVIS radiance levels, and, as observed with the unaided eye, this decline is less obvious at low light levels (figs. 18–20). The peripheral acuity is less affected by target radiance than is foveal acuity.

Comparison of Unaided and Intensified Vision

The description of VA while using the image intensifiers has little meaning on its own since most of us are unaware of the significance of each NVIS radiance

level. Few know the NVIS radiance expected from viewing a tree under starlight, or the environmental significance of 1×10^{-8} W/sr·m^2. Therefore, the real significance of these findings becomes apparent only when we compare aided and unaided vision for a given environmental lighting condition.

Tables 1 and 2 show luminance (candles per square meter) and NVIS radiance (in Gen III weighted satts per sterandian·meters squared) of the laboratory test conditions (table 1) and a select set of representative nocturnal environmental lighting conditions (table 2). Figure 21 shows the relationship between these two data sets. In the top half of figure 21, the sampled VA versus display luminance function is plotted. Symbols below the data set show luminance levels for two targets (100% reflector and green foliage) expected for the representative night-sky conditions. It can be seen that we were able to measure acuities over luminance ranges that encompass FM, 50%M and 20%M, but acuity fell below levels we could measure (20/400) at luminance values equivalent to SL and CSL.

Quite a different trend can be seen in the bottom half of figure 21, where VA is plotted against NVIS radiance. We were able to measure acuity at radiance levels below that expected from CSL. Interestingly, because of an underestimate of the radiance provided by the FM, our highest test level was slightly lower than that expected from a full moon at 90° elevation.

Figure 22 shows the interpolation procedure used to determine VA expected for a given environmental condition. Simple linear interpolation techniques were employed. In some cases, we also used small amounts (less than half log unit) of extrapolation beyond the experimental data range to estimate VA for high or very low light levels.

Using the interpolation techniques described above, we are now able to plot both the aided and unaided acuity data on a common axis. These data are plotted in figures 23–26. The horizontal scale is not linear, but represents five nocturnal lighting conditions (FM, 50%M, 20%M, SL, and CSL). Intensified data are shown as circles and unintensified data as squares. The improvement in vision provided by the NVG is evident at all of the nocturnal light levels used here.

Foveal acuity (figure 23) is improved the most by intensification. High-contrast acuity (top panel) is significantly elevated at FM (0.15 log units) and even more at 50%M (>1 log unit). Also, the NVG provides acuities at the lowest light levels (CSL) that can be superior to those obtainable at the brightest possible night illumination conditions (FM). This is particularly striking for the case of a green foliage reflector, because this target selectively reflects light in the near-IR. For such a target, intensified high-contrast visual acuity under CSL conditions exceeds that of unaided acuity under FM conditions by a factor of 2. The discrepancy is not so large for targets with uniform reflection spectra (open symbols). Also, image intensification makes many targets resolvable that are simply invisible to the unaided eye. For example, unaided foveal acuity for low-contrast (10% contrast) targets was unmeasurable for all nocturnal lighting conditions. However, with the aid of the NVG, low-contrast acuities ≤20/200 were observed for all but the very lowest light levels.

Similar trends can be seen in the 5° eccentric data (fig. 24), 10° eccentric data (fig. 25) and 20° eccentric data (fig. 26). However, one important trend can be seen when comparing these different eccentricities. When comparing the high-contrast acuity data (top panels), the improvements provided by intensification are reduced as eccentricity is increased. It is difficult to observe this trend in the lower-contrast data because many of these lower-contrast stimuli become invisible.

This eccentricity dependence is shown clearly in figures 27 and 28, where VA is plotted as a function of target eccentricity for a variety of light levels. Figure 27 shows visual acuity on a linear scale; in figure 28, the same data are replotted on a log acuity scale.

In these figures, photopic VA is plotted as a reference (filled circles), and the classic foveal acuity peak is seen. However, in viewing targets that have low reflectances within the visible spectrum (e.g., green foliage), nocturnal acuities show no foveal peak. Full-moon data show almost uniform acuity across the central 20° (filled squares), and the 50%M data actually show a central scotoma (filled diamonds) where no acuity could be measured.

Foveal acuity with the NVG fails to show the very pronounced foveal peak (fig. 27 open and shaded symbols), but clearly shows superior vision foveally for all lighting conditions. Most notable is the observation that although the unaided fovea loses most at low light levels, it also gains most by intensification. Unaided acuity at 20° in the periphery only benefits slightly from intensification, but sufficient to allow more stimuli to be visible at lower light levels than possible in the unaided condition (see fig. 26).

Discussion

This study has developed an alternative experimental model for examining human visual capabilities while using image intensification. Rather than try to mimic the radiometric spectrum of the night sky in the laboratory, an arbitrary spectral source is used and its

integral is matched to that of selected nocturnal environmental conditions. This requires a rather simple model that includes the spectral properties of both the laboratory stimulus and the nocturnal environment (irradiance and reflectance). The main advantage of this approach is its flexibility, since any laboratory stimulus can be used. In order to test this approach, a study was performed to examine the effect of light level on VA foveally and peripherally. The results provide clear indications of the value of NVGs for night operations and show that the benefits afforded by the NVGs, although most pronounced in the fovea, are observed over a fairly wide region of the visual field. The results also show that the superiority of binocular vision over monocular vision, although quite small for VA, is similar for intensified and unintensified vision.

The precipitous decline in foveal acuity observed as retinal illuminance approaches cone absolute thresholds (0.1 trolands) seen in figure 10, and the absolute central scotoma that accompanies further reductions effectively disable humans at all nocturnal light levels. For most of us, this disability can be easily accommodated by technology that introduces artificial lighting, as well as by behavioral changes. However, there are specific tasks that must be carried out irrespective of the time of day or night that cannot be accompanied by artificial light sources. Because of these demands, image intensification technology is an important tool. Very simply, with the use of large apertures, photomultipliers, and microchannel plates, the photon flux entering the eye (and, consequently, retinal illuminance) can be increased dramatically (several thousand times). The rationale is that any decrements in image quality introduced by the image intensification system will be small relative to the vast improvements in neural image quality introduced by the increase in retinal illuminance.

There are numerous scientific, casual, and field observations to confirm that modern image intensifiers can provide dramatic improvements in human visual performance under low mesopic/scotopic conditions, in spite of potential reductions in image quality. However, no systematic evaluation of intensified vision or retinal image quality has been performed, and little is known of the visual capabilities and limitations of these instruments. This paucity of quality data may stem from the choice of experimental models, which have required most studies to employ rather inferior methods and a very restricted range of experiments. The experimental model employed in the present study will allow a complete documentation of the visual capabilities of these instruments.

The acuity data presented herein confirm some previous findings that show that intensified foveal vision exceeds that of unintensified vision over most of the nocturnal range (Full moon illumination and below, figs. 23–26). Clearly, such findings support the use of Gen III NVGs during night operations. Our data also show that the benefits of intensification are more pronounced for lower-contrast targets. The results shown in figures 23–26 also emphasize the significant effect of the source and reflection spectra. The practical improvement in vision provided by the NVGs may be significantly underestimated if a white reflector is used (most previous studies use such a reflector). Of particular significance is the visual improvements demonstrated over a wide range of eccentricities.

References

1. Hoover, K.: Visual Acuity with the ITT Night Vision Aid for Patients with Night Blindness. American Journal of Optometry and Physiological Optics, vol. 60, 1983, pp. 762–768.
2. Wiley, R.; Glick, D.; and Holly, F.: AN/PVS-5 Night Vision Goggles. U.S. Army Aviation Digest, May 1983, pp. 1–6.
3. Levine, R.; and Rash, C.: Visual Acuity with AN/PVS-5A Night Vision Goggles and Simulated Flashblindness Protective Lenses Under Varying Levels of Brightness and Contrast. USAARL 89-16, Fort Rucker, Ala, 1989.
4. Wiley, R.: Visual Acuity and Stereopsis with Night Vision Goggles. USAARL 89-9, Fort Rucker, Ala., 1989.
5. Wilkinson, M.; and Bradley, A.: Night Vision Goggles: An Analysis of Dynamic Range and Visual Performance for the Unaided and NVG-Aided Eye. Tri-Service Command, St. Louis, Mo., 1989.
6. Kotulak, J.; and Rash, C.: Visual Acuity with Second and Third Generation Night Vision Goggles Obtained from a New Method of Night Sky Simulation Across a Wide Range of Target Contrast. USAARL 92-9, Fort Rucker, Ala., 1992.
7. Wilkinson, M.; Thibos, L.; and Bradley, A.: Neural Basis of Scotopic Acuity. Invest. Ophthalmol., vol. 32, 1991, p. 699.
8. Still, D.; Temme, L.; Huckabone, M.; and Mittelman, M.: Visual Limitations of NVDs. Tri-Service Command, Ariz., 1991.

9. Wiley, R.; and Holly, F.: "Vision with the AN/PVS-5 Night Vision Goggles." AGARD Conference Proceedings 191, Neuilly Sur Seine, France, 1976.

10. Vatsia, M.; Stich, U.; and Dunlap, D.: Night Sky Radiant Sterance From 450 to 2000 Nanometers. Report ECOM-7022, United States Army Electronics Command, 1972.

11. Hood, D.; and Finklestein, M.: Visual Sensitivity. Handbook of Perception and Human Performance, vol. 1, K. Boff, L. Kaufman, and J. Thomas, eds., Wiley, New York, 1986.

12. Electro-Optics Handbook. Radio Corporation of America, Burlington, Mass., 1968.

13. Stefanik, R.: Night Sky Radiometric Measurements during Follow-On Evaluation Testing of AN/PVS-7 (A,B) at Fort Benning, Georgia. AMSEL-NV-TR-0079, Center for Night Vision and Electro-Optics, 1989.

14. Ginsburg, A.; Easterly, J.; and Evans, D.: Contrast Sensitivity Predicts Target Detection Field Performance of Pilots. Proceedings of the Human Factors Society, 1983, pp. 269–273.

15. Kruk, R.; and Regan, D.: Visual Test Results Compared with Flying Performance in Telemetry-Tracked Aircraft. Aviation, Space, and Environmental Medicine, vol. 54, 1983, pp. 906–911.

16. Kruk, R.; Regan, D.; Beverley, K.; and Longridge, T.: Correlations between Visual Test Results and Flying Performance on the Advanced Simulator for Pilot Training (ASPT). Aviation, Space and Environmental Medicine, vol. 52, 1981, pp. 455–460.

17. O'Neal, M.; and Miller, R.: Further Investigation of Contrast Sensitivity and Visual Acuity in Pilot Detection of Aircraft. AAMRL-TR-88-002, USAF School of Aerospace Medicine, San Antonio, Tex., 1988.

18. Shinar, D.; and Gilead, E.: Contrast Sensitivity as a Predictor of Complex Target Detection. Proceedings of the Human Factors Society, 1987, pp. 1194–1197.

19. Task, H.; and Pinkus, A.: Contrast Sensitivity and Target Recognition Performance: A Lack of Correlation. SID Digest, 1987, pp. 127–130.

20. Kerr, J.: Visual Resolution in the Periphery. Perception and Psychophysics, vol. 9, 1971, pp. 375–378.

21. Bradley, A.; Hook, J.; and Haeseker, J.: A Comparison of Clinical Acuity and Contrast Sensitivity: Effect of Uncorrected Myopia. Ophthalmic Physiol Optics, vol. 11, 1991, pp. 218–226.

22. Hecht, S.: The Relation between Visual Acuity and Illumination. J. Gen. Physiol., vol. 11, 1928, pp. 255–281.

23. Shlaer, S.: The Relation between Visual Acuity and Illumination. J. Gen. Physiol., vol. 21, 1937, pp. 165–188.

24. Hecht, S.; and Mintz, E.: The Visibility of Single Lines at Various Illuminations and the Retinal Basis of Visual Resolution. J. Gen. Physiol., vol. 22, 1939, pp. 593–612.

25. Shlaer, S.; Smith, E.; and Chase, A.: Visual Acuity and Illumination in Different Spectral Regions. J. Gen. Physiol., vol. 25, 1942, pp. 55–569.

26. Mandelbaum, J.; and Sloan, L.: Peripheral Visual Acuity. Am. J. Ophthalmol., vol. 30, 1947, pp. 581–588.

27. Sloan, L.: The Photopic Acuity-Luminance Function with Special Reference to Parafoveal Vision. Vision Research, vol. 8, 1968, pp. 901–911.

28. Campbell, F.; and Green, D.: Monocular versus Binocular Visual Acuity. Nature (London), vol. 208, 1965, pp. 191–2.

Table 1. Luminances, radiances, and Nvis radiances available during experiment

ND filter	Luminance, cd/m^2	NVIS radiance, W/sr·m^2	Radiance, W/sr·m^2
0.0	120.0	0.00435816	0.47308585
0.5	37.95	0.00137817	0.14960288
1.0	12.00	0.00043582	0.04730859
1.5	3.79	0.00013782	0.01496029
2.0	1.20	4.3582E-05	0.00473086
2.5	0.3795	1.3782E-05	0.00149603
3.0	0.12	4.3582E-06	0.00047309
3.5	0.03795	1.3782E-06	0.0001496
4.0	0.012	4.3582E-07	4.7309E-05
4.5	0.003795	1.3782E-07	1.496E-05
5.0	0.0012	4.3582E-08	4.7309E-06
5.5	0.0003795	1.3782E-08	1.496E-06
6.0	0.00012	4.3582E-09	4.7309E-07

Note: The unfiltered P4 phosphor display has a luminance of 120 cd/m^2. NVIS radiances include the near IR and red filter. Integrals are calculated from 380-760 nm.

Table 2. Representative values of visible radiance (luminance) and Nvis radiance for several "standard" night sky condition

	Luminance, cd/m^2		NVIS radiance, W/sr·m^2	
	White paper	Green leaves	White paper	Green leaves
FM	0.07961783	0.00992923	0.00018723	8.0502E-05
50%M	0.00605096	0.00075462	1.423E-05	6.1181E-06
20%M	0.00101911	0.00012609	3.3273E-06	1.5924E-06
SL	0.00031847	3.9917E-05	1.9515E-06	1.0722E-06
CSL	3.1847E-05	3.9298E-06	1.3792E-07	7.2251E-08

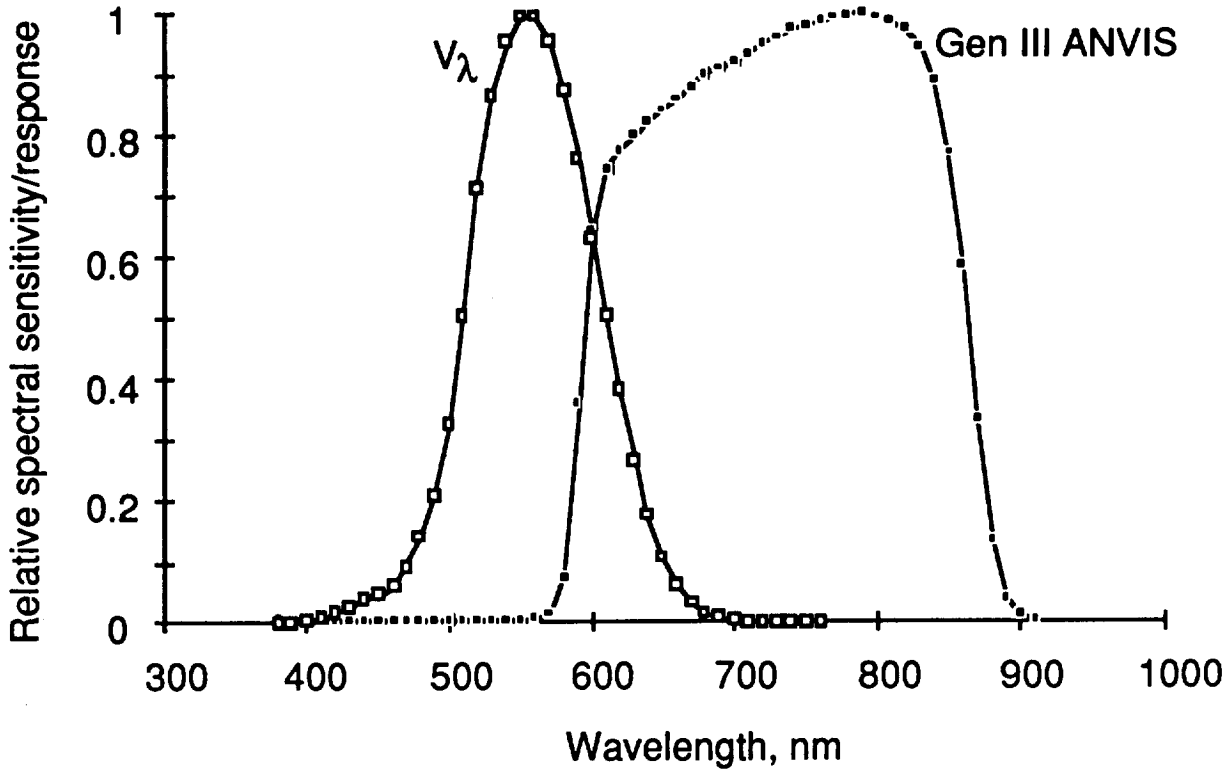

Figure 1. Plot of relative spectral sensitivities of human eye under photopic conditions (open squares) and spectral response of ITT Gen III image intensifier tube (filled squares).

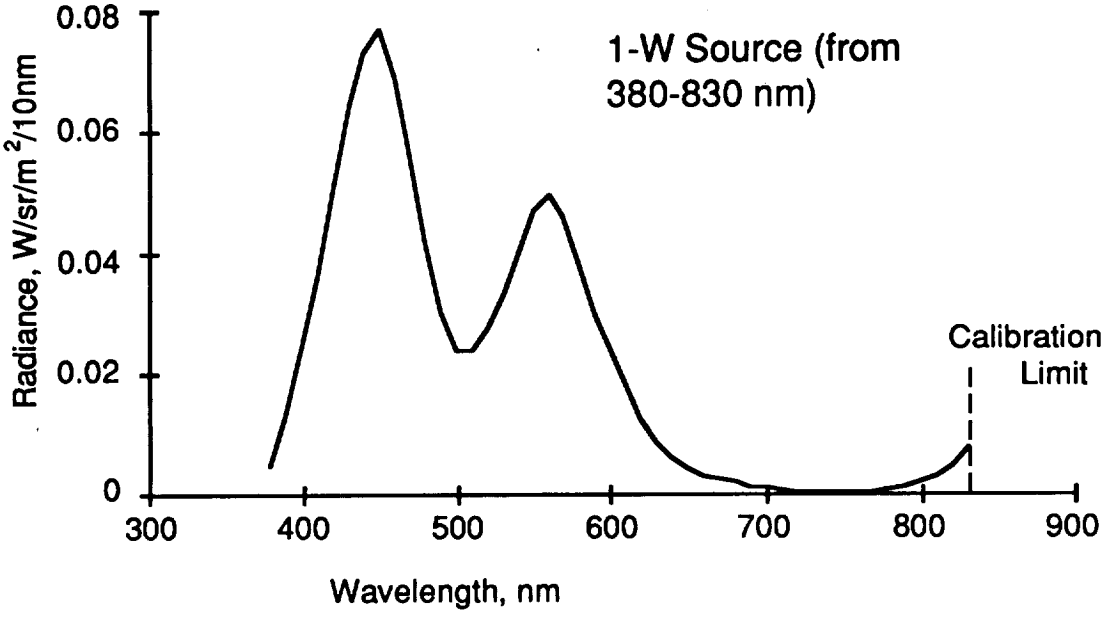

Figure 2. Radiance spectrum for P4 phosphor display (Macintosh Gray-scale monitor).

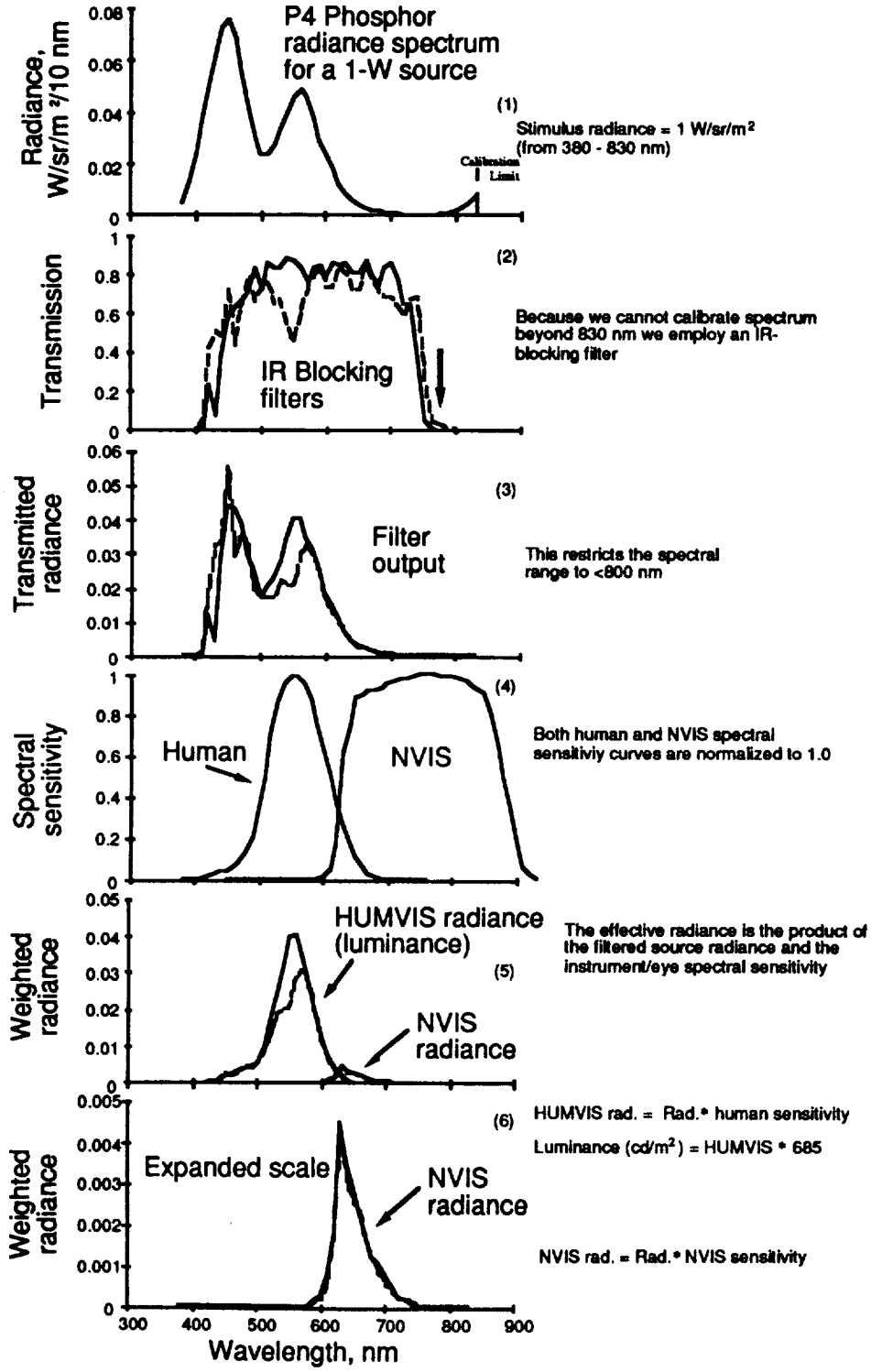

Figure 3. Schematic representation of the calculation of luminance and NVIS radiance of our display monitor.

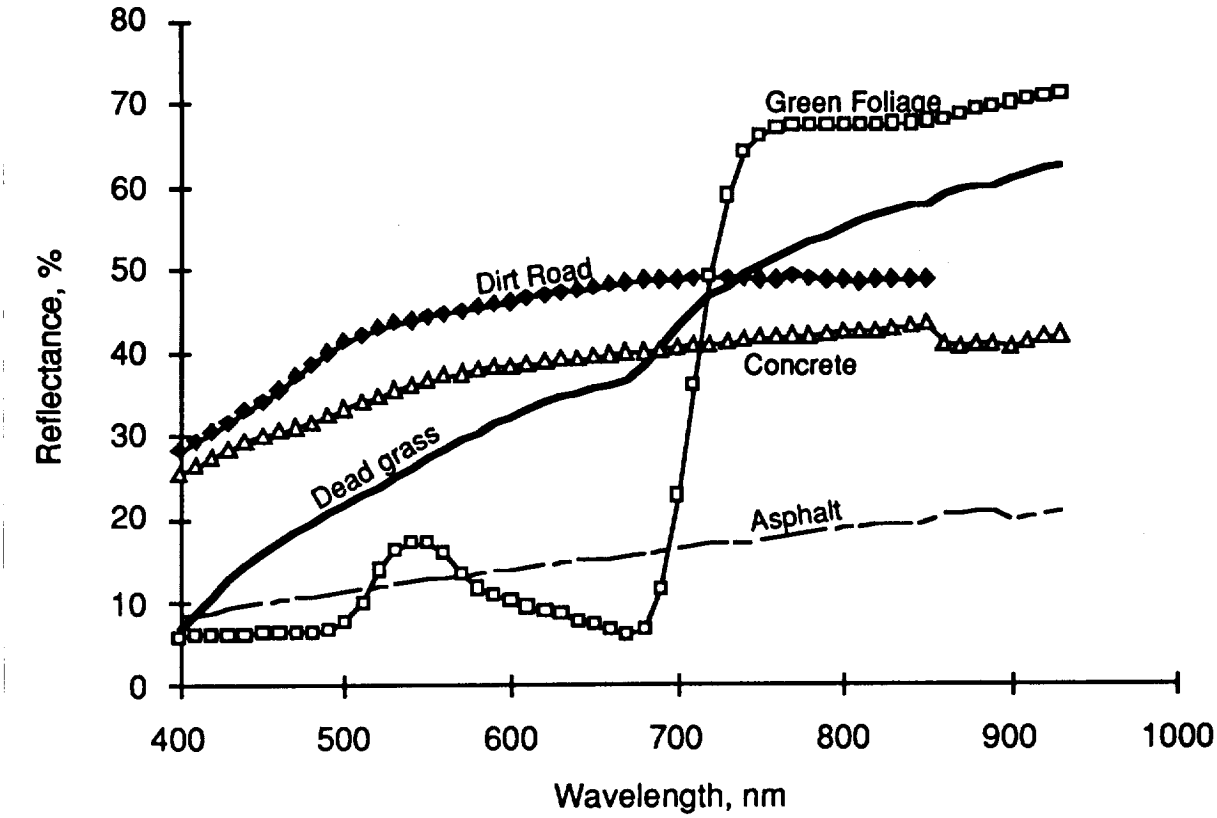

Figure 4. Reflection spectra of five commonly encountered materials plotted as percentage of incident radiation reflected at each wavelength.

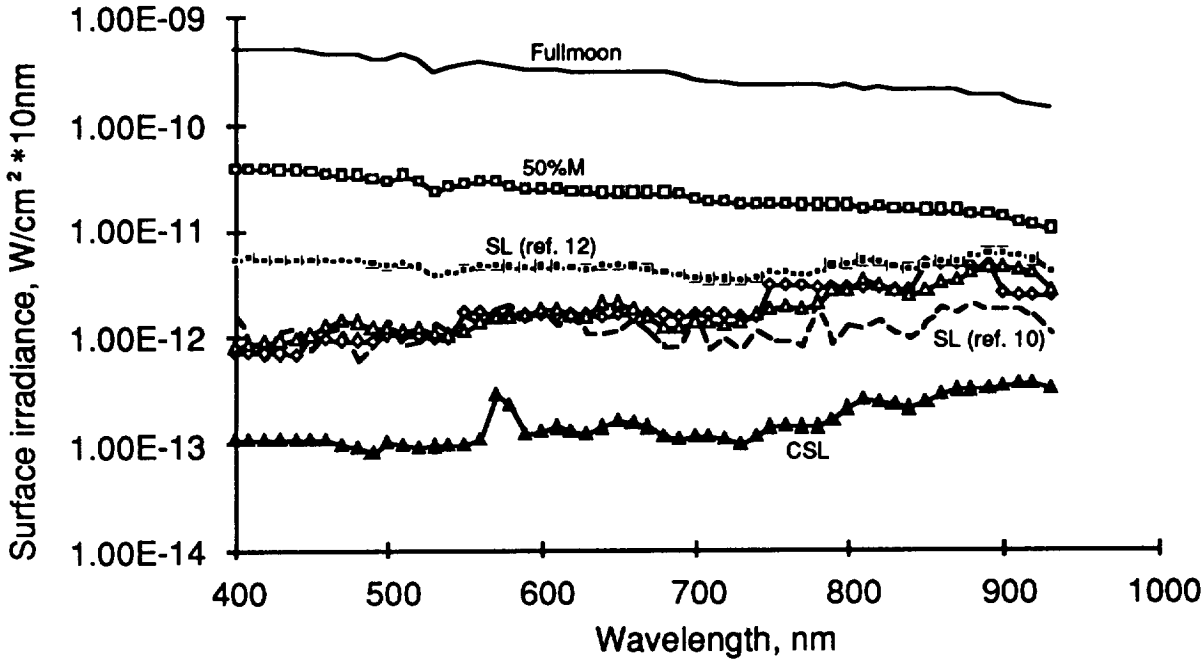

Figure 5. Earth surface irradiance spectra for a variety of night illumination conditions.

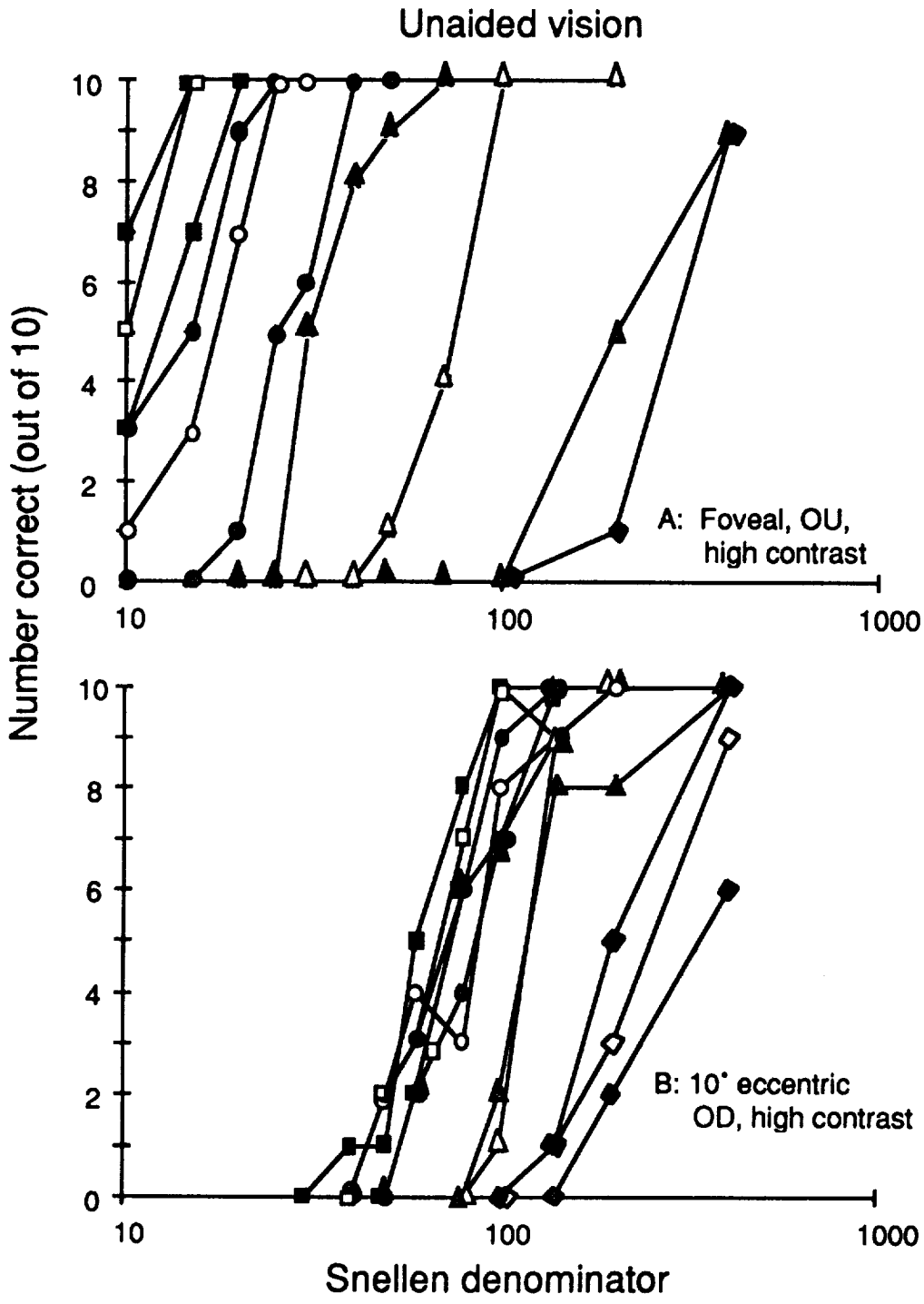

Figure 6. Sample psychometric functions obtained with unaided vision both centrally and peripherally.

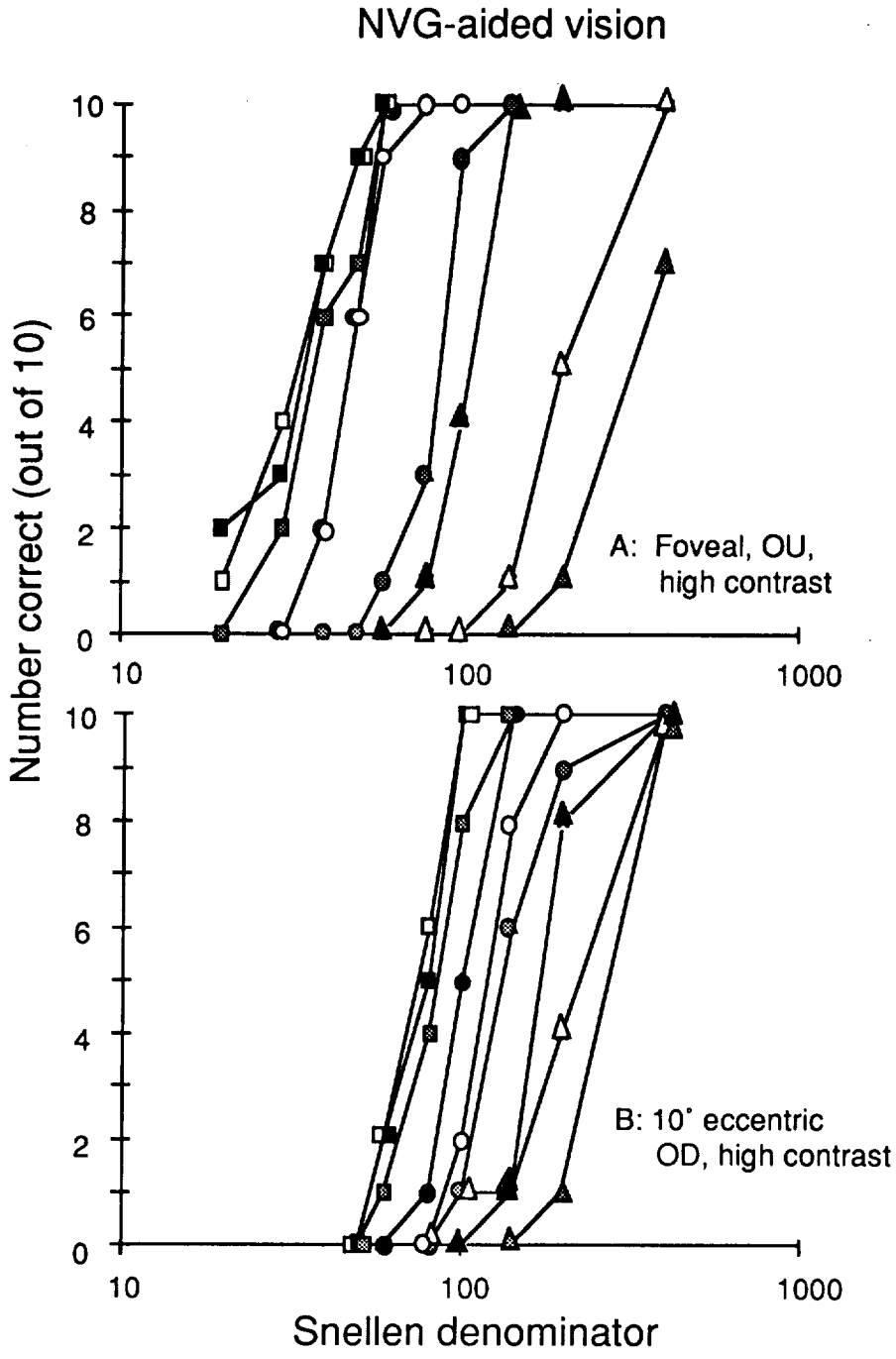

Figure 7. Same as figure 6 except with NVG vision.

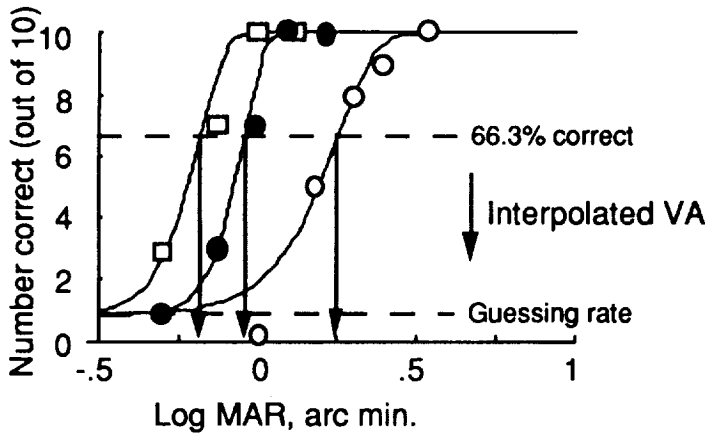

Figure 8. Example of curve fitting procedure used to estimate VA (expressed as the log of monocular angular resolution (MAR) by interpolation).

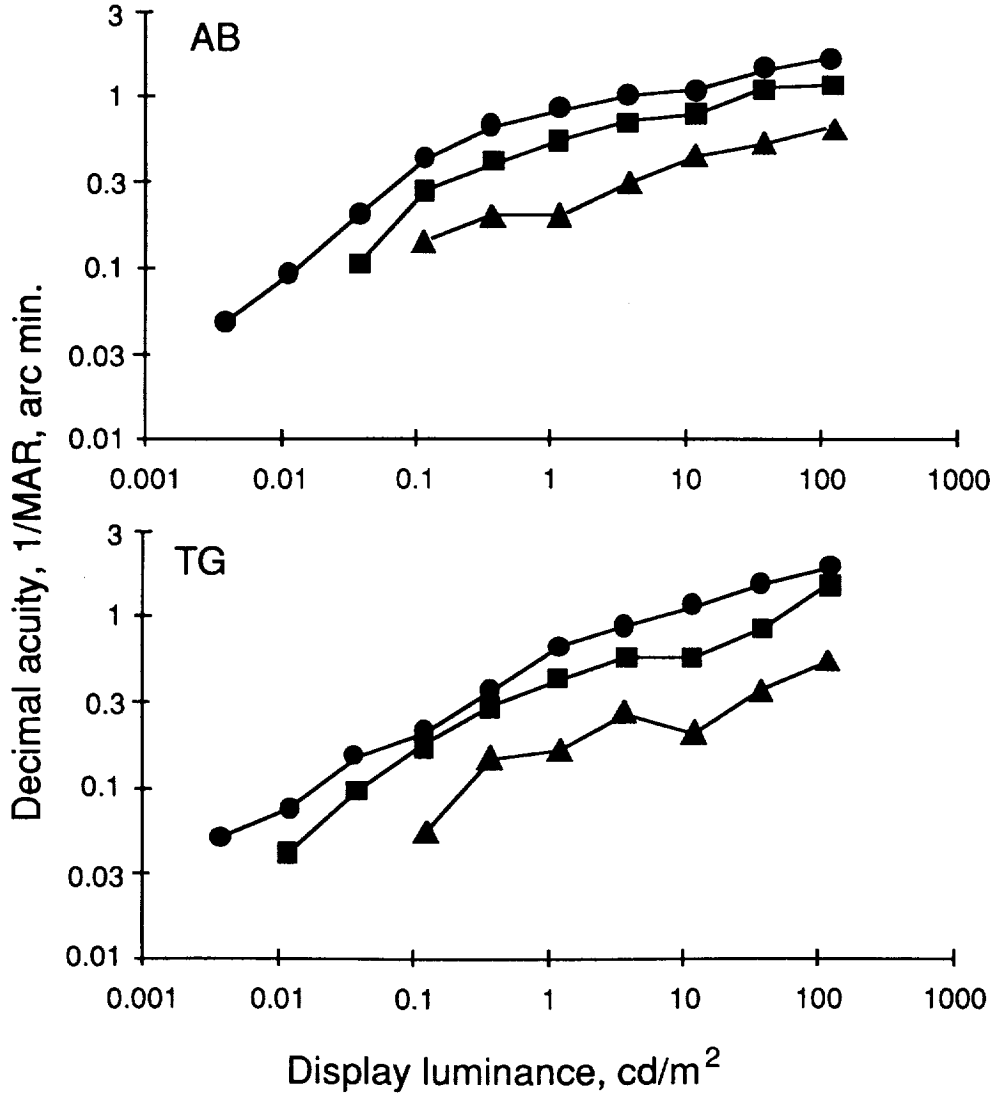

Figure 9. Unaided VA as function of target luminance for two subjects (AB and TG).

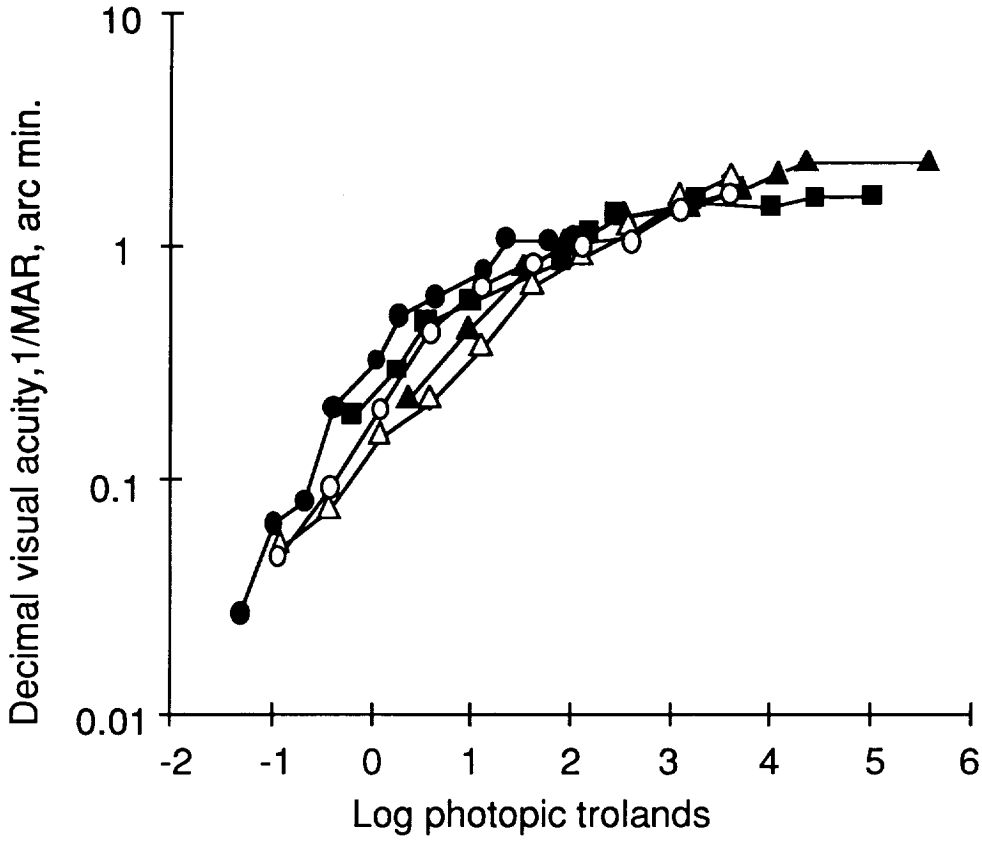

Figure 10. Comparison of high-contrast unaided VA data from this study (open symbols) with those measured in earlier studies.

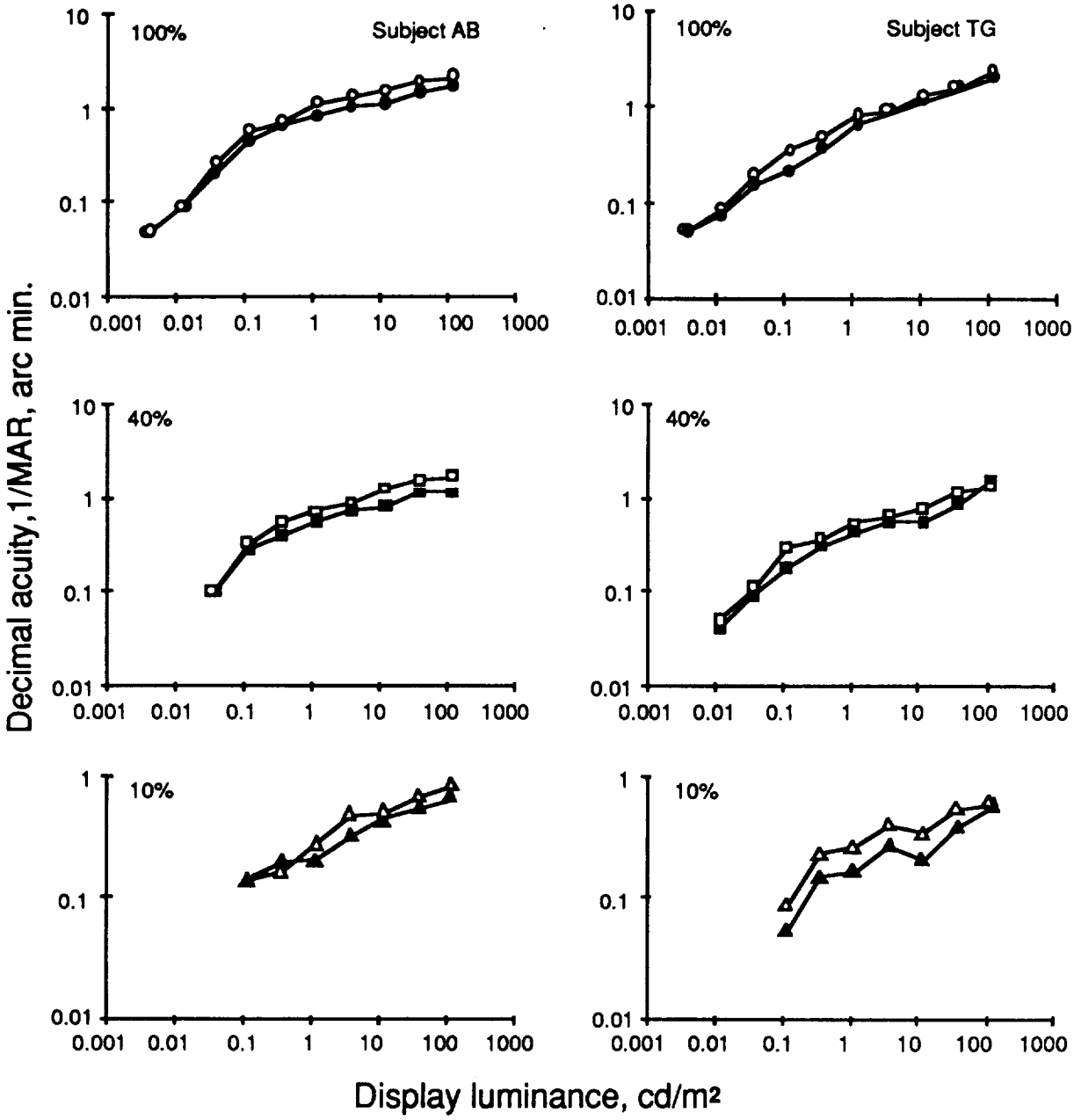

Figure 11. Monocular (filled symbols) and binocular (open symbols) unaided acuities for two subjects at three letter contrasts.

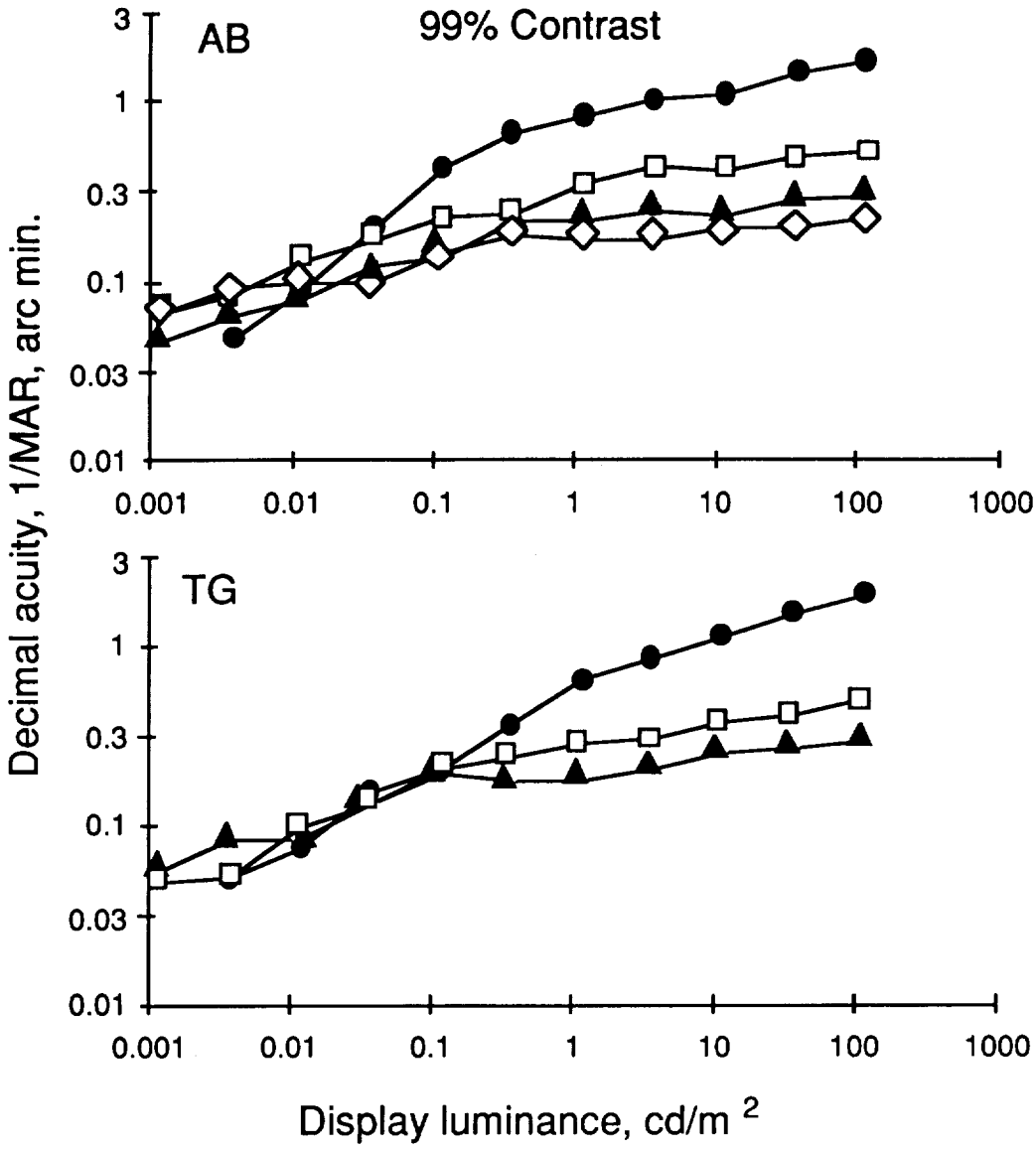

Figure 12. Unaided high (99%) contrast VA as function of target luminance for two subjects.

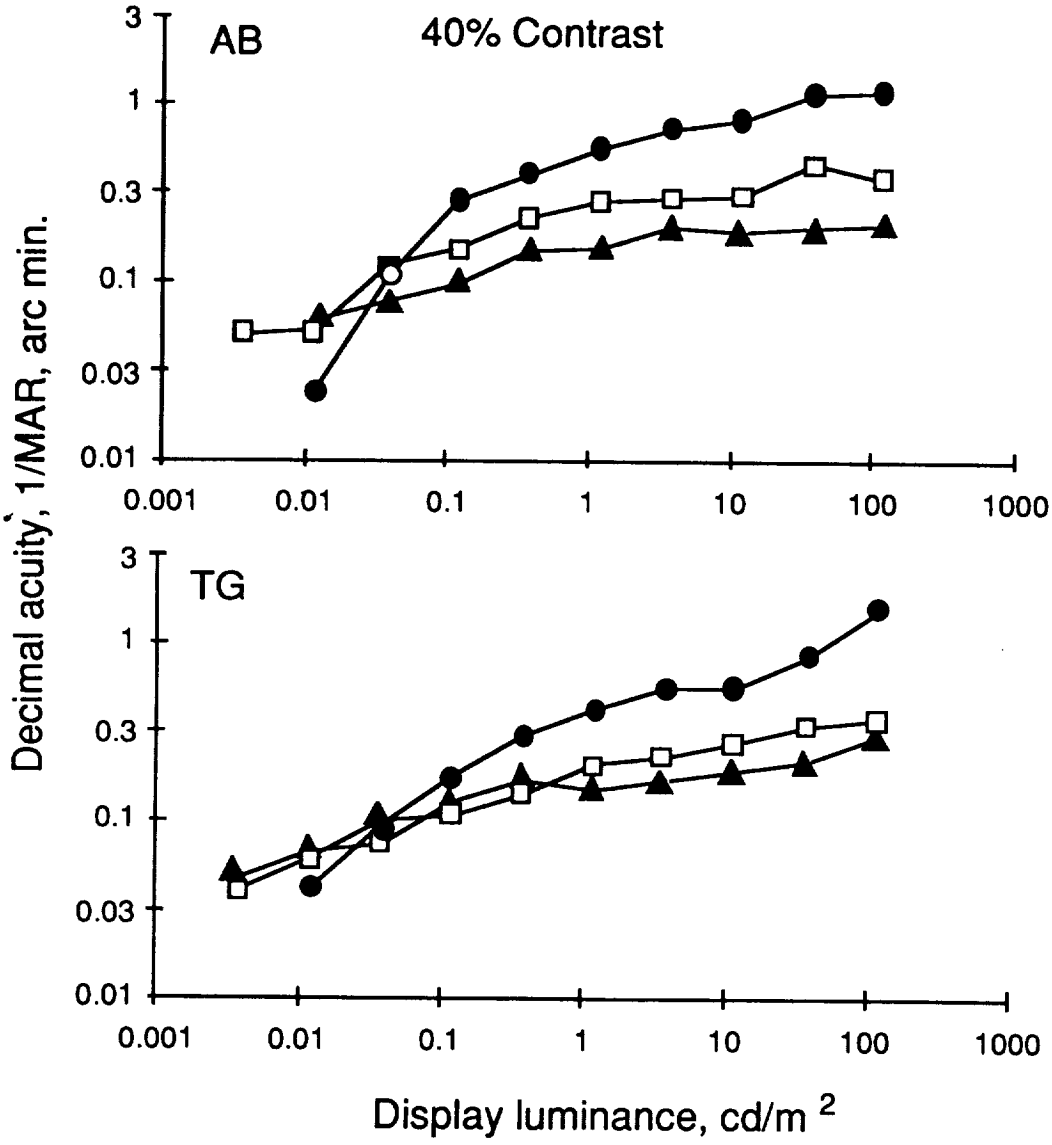

Figure 13. Unaided medium (40%) contrast VA as function of target luminance for two subjects.

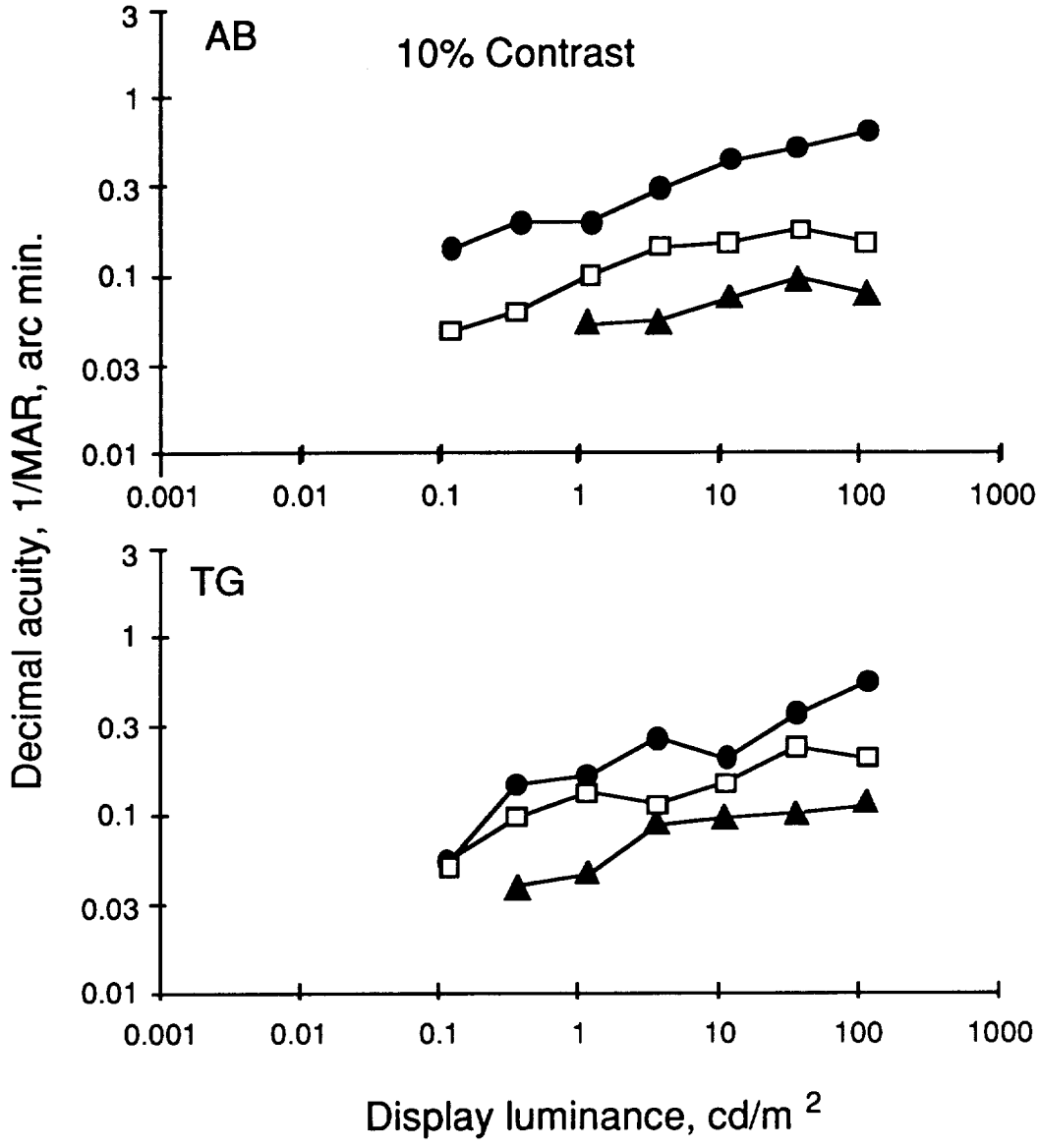

Figure 14. Unaided low (10%) contrast VA as function of target luminance for two subjects.

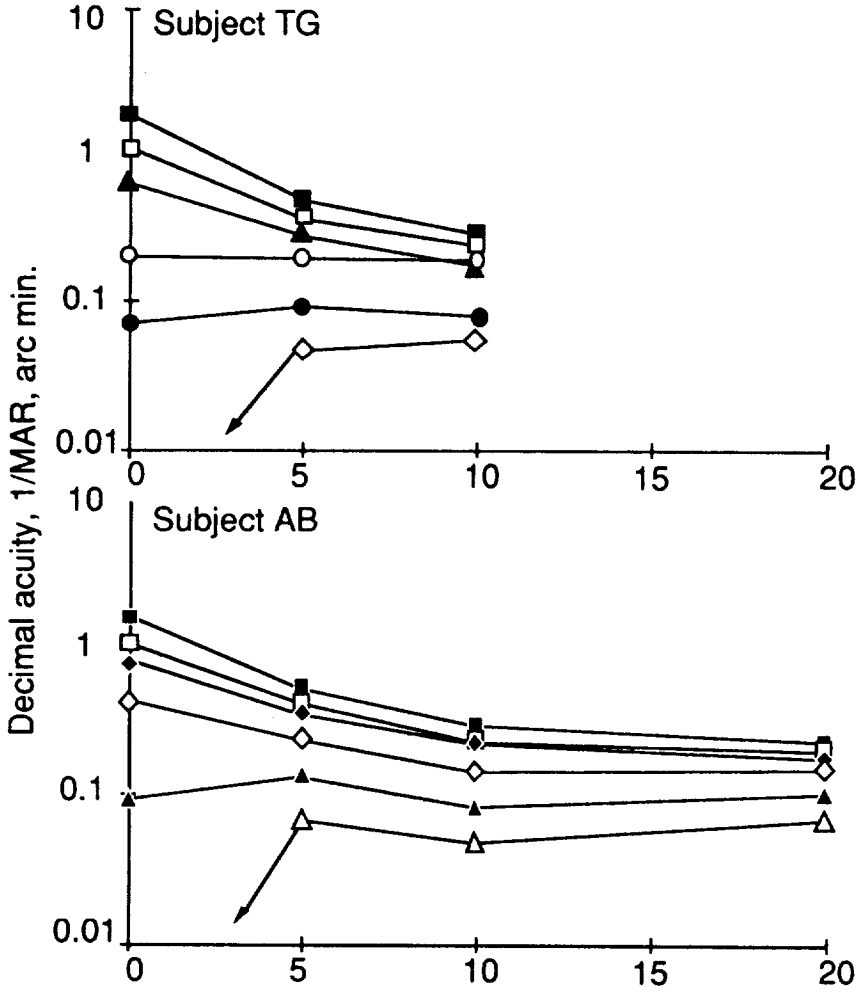

Figure 15. VA as function of target eccentricity for a range of target luminances.

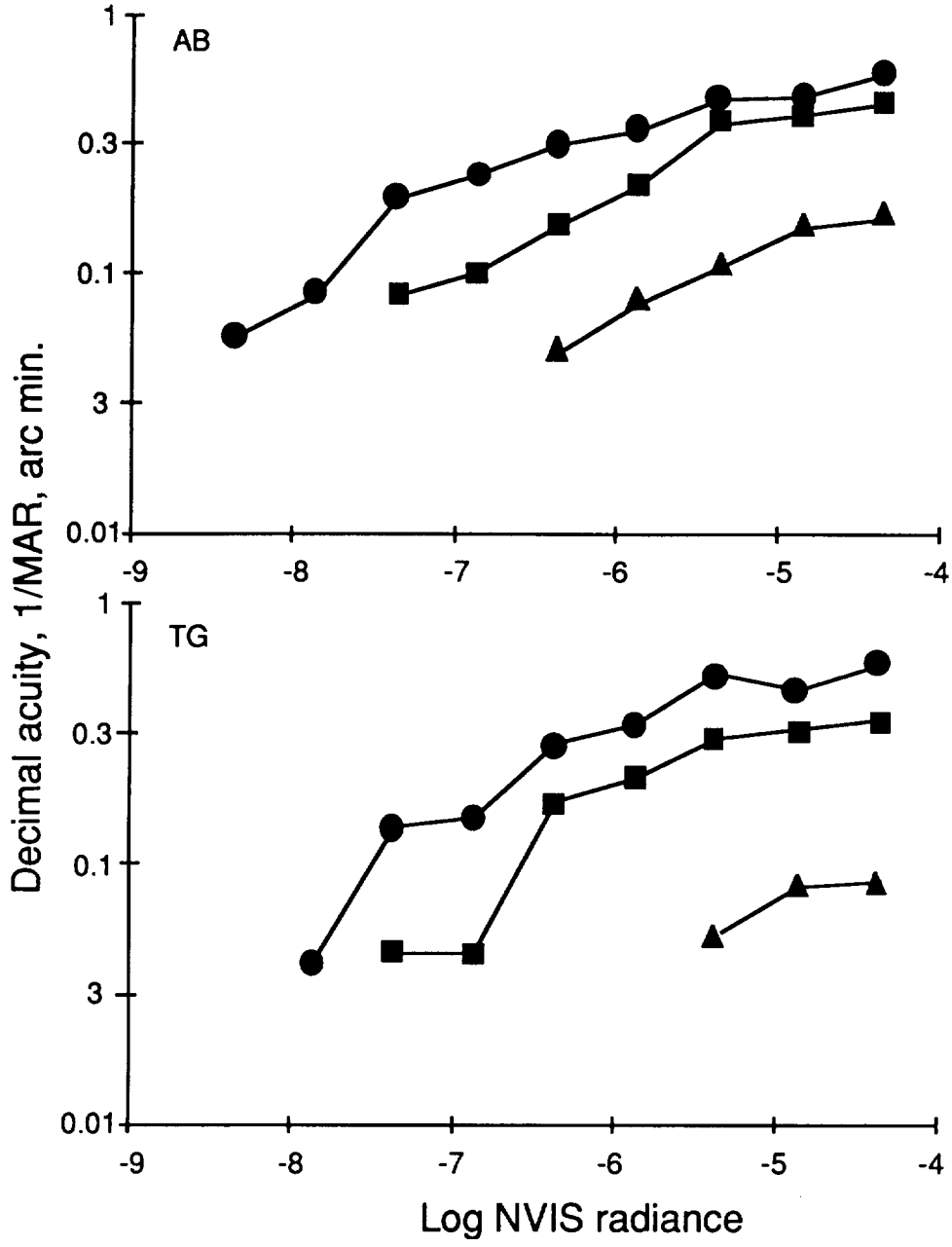

Figure 16. NVG-aided VA as function of target radiance (NVIS radiance) for two subjects (AB and TG).

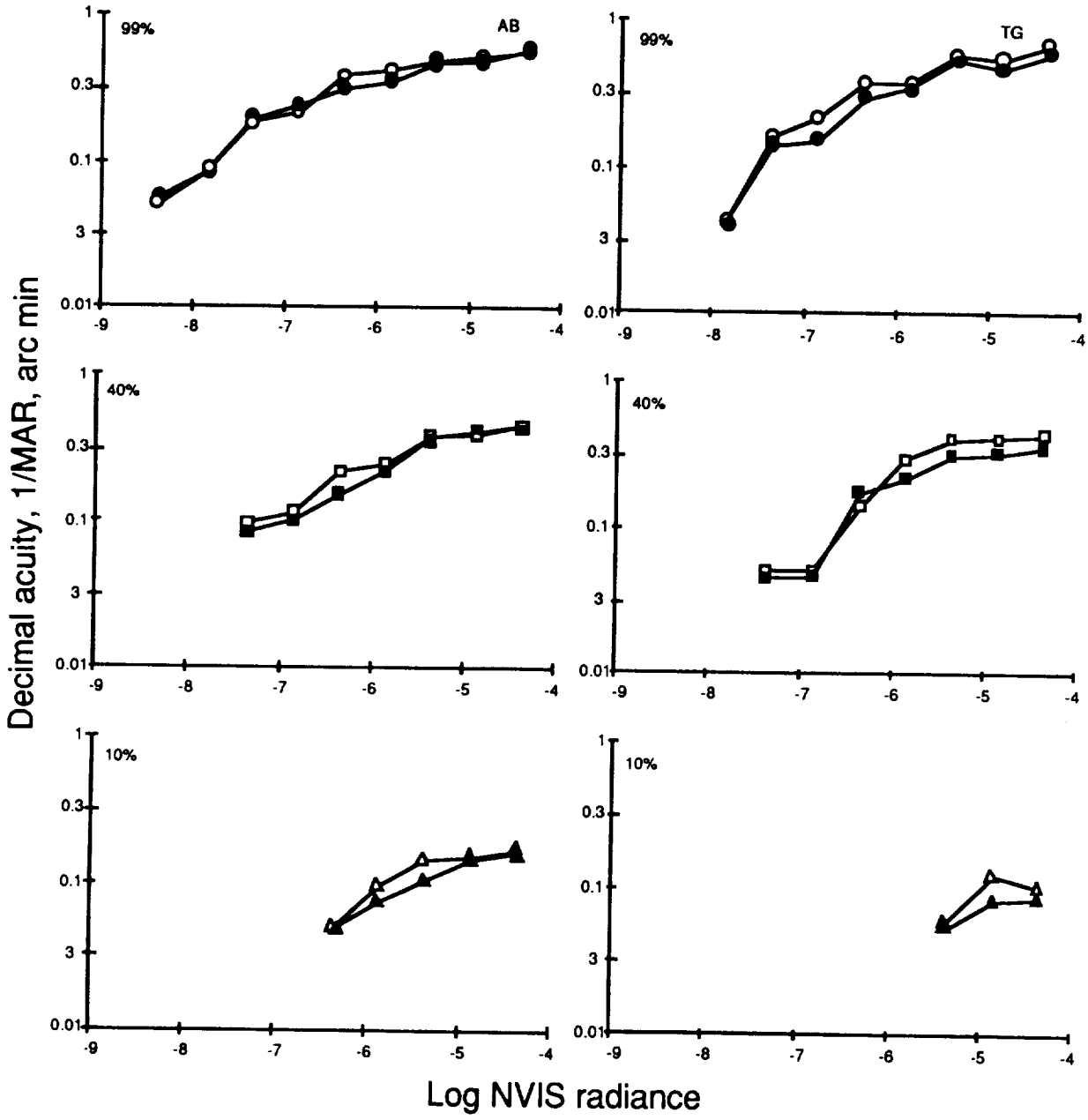

Figure 17. Monocular (filled symbols) and binocular (open symbols) NVG-aided acuities for two subjects at three letter contrasts.

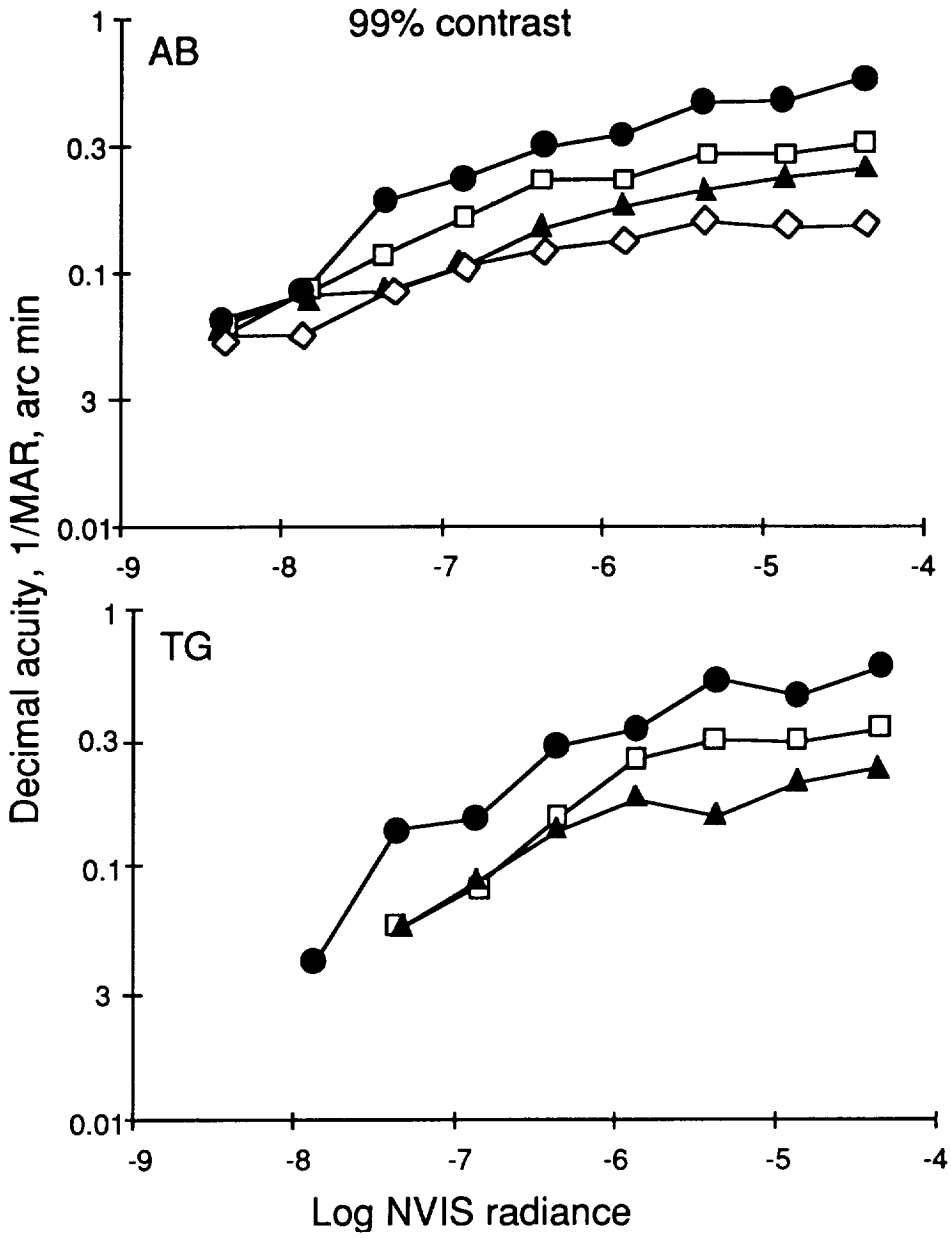

Figure 18. Unaided high (99%) contrast NVG-aided VA as function of target luminance for two subjects.

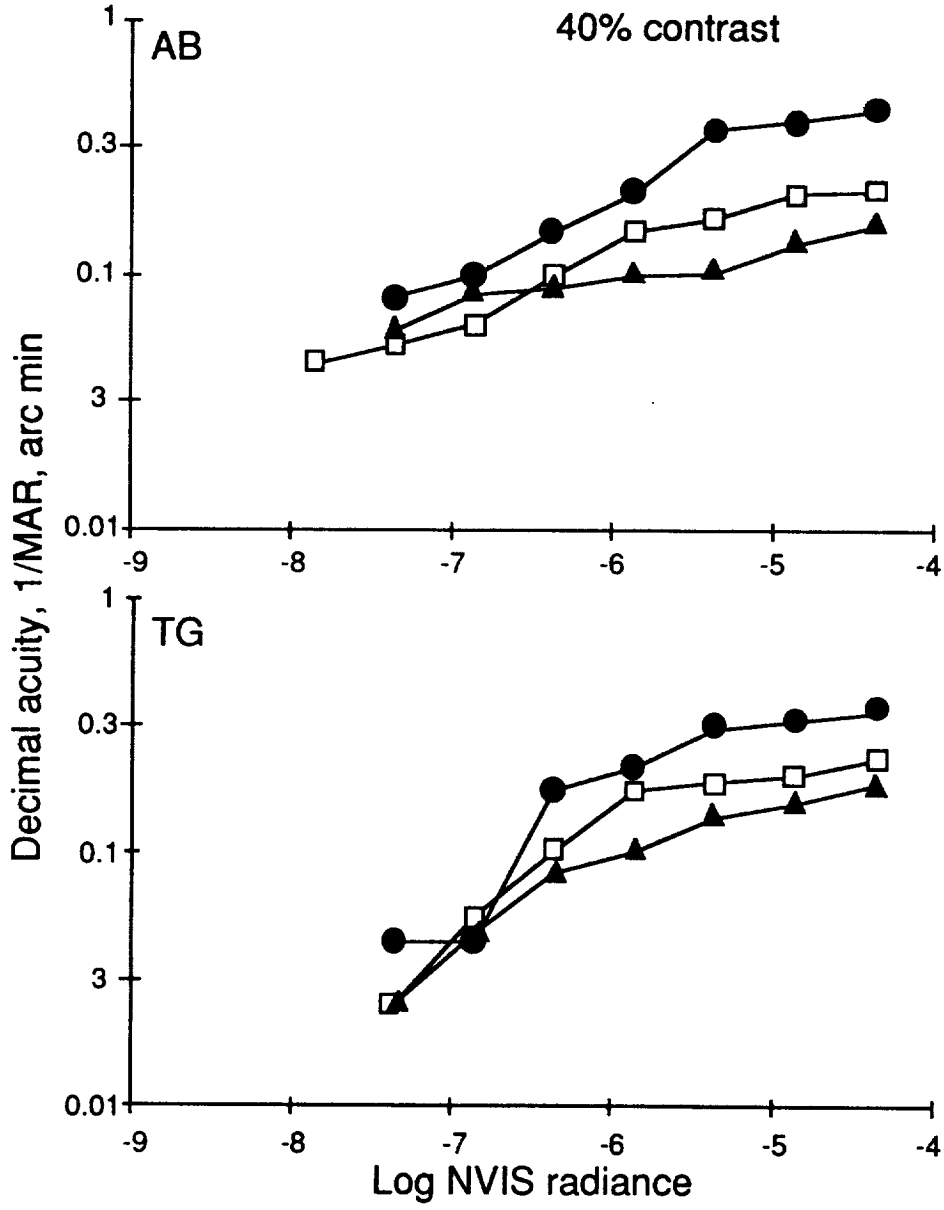

Figure 19. Unaided medium (40%) contrast NVG-aided VA as function of target luminance for two subjects.

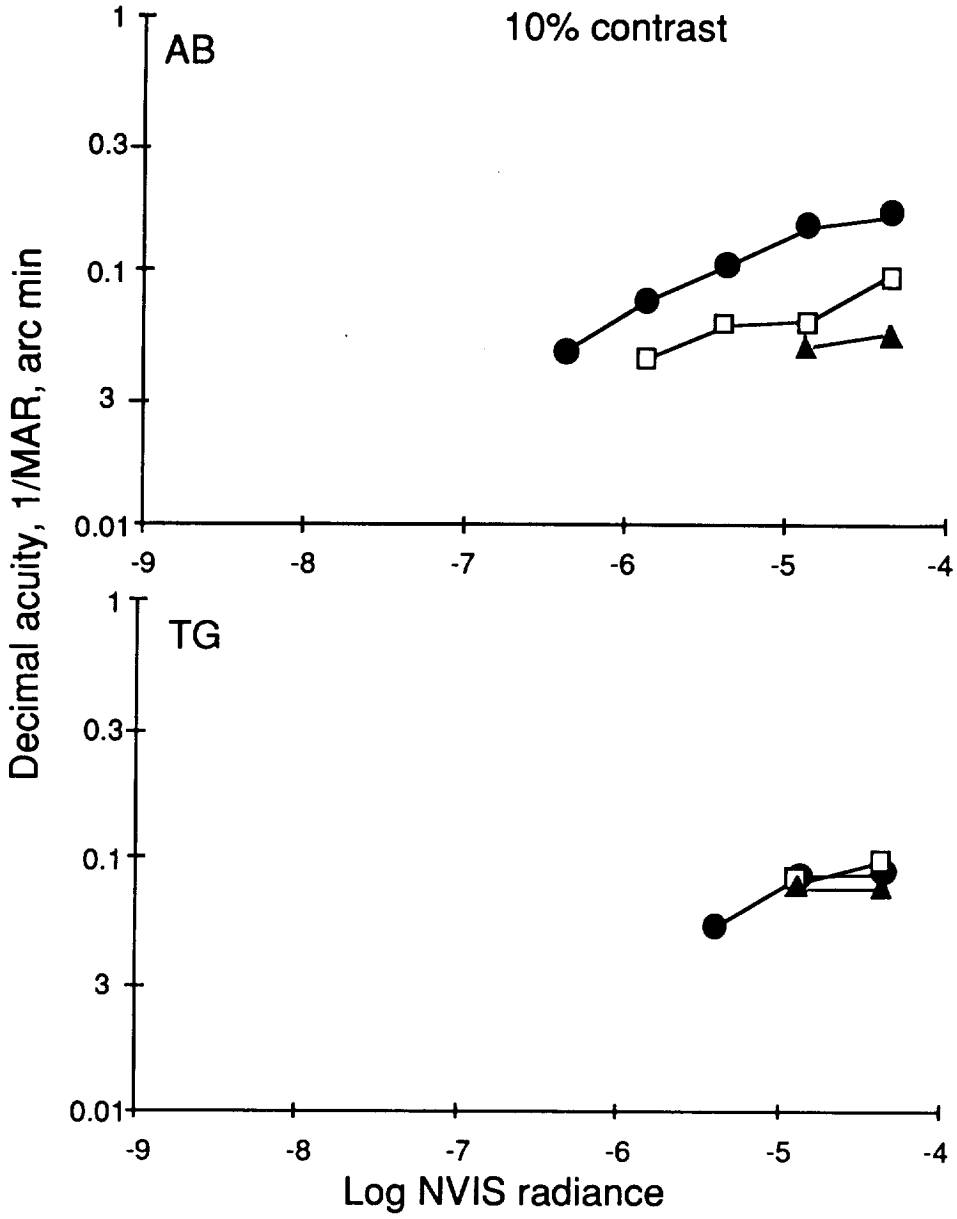

Figure 20. Unaided low (10%) contrast NVG-aided VA as function of target luminance for two subjects.

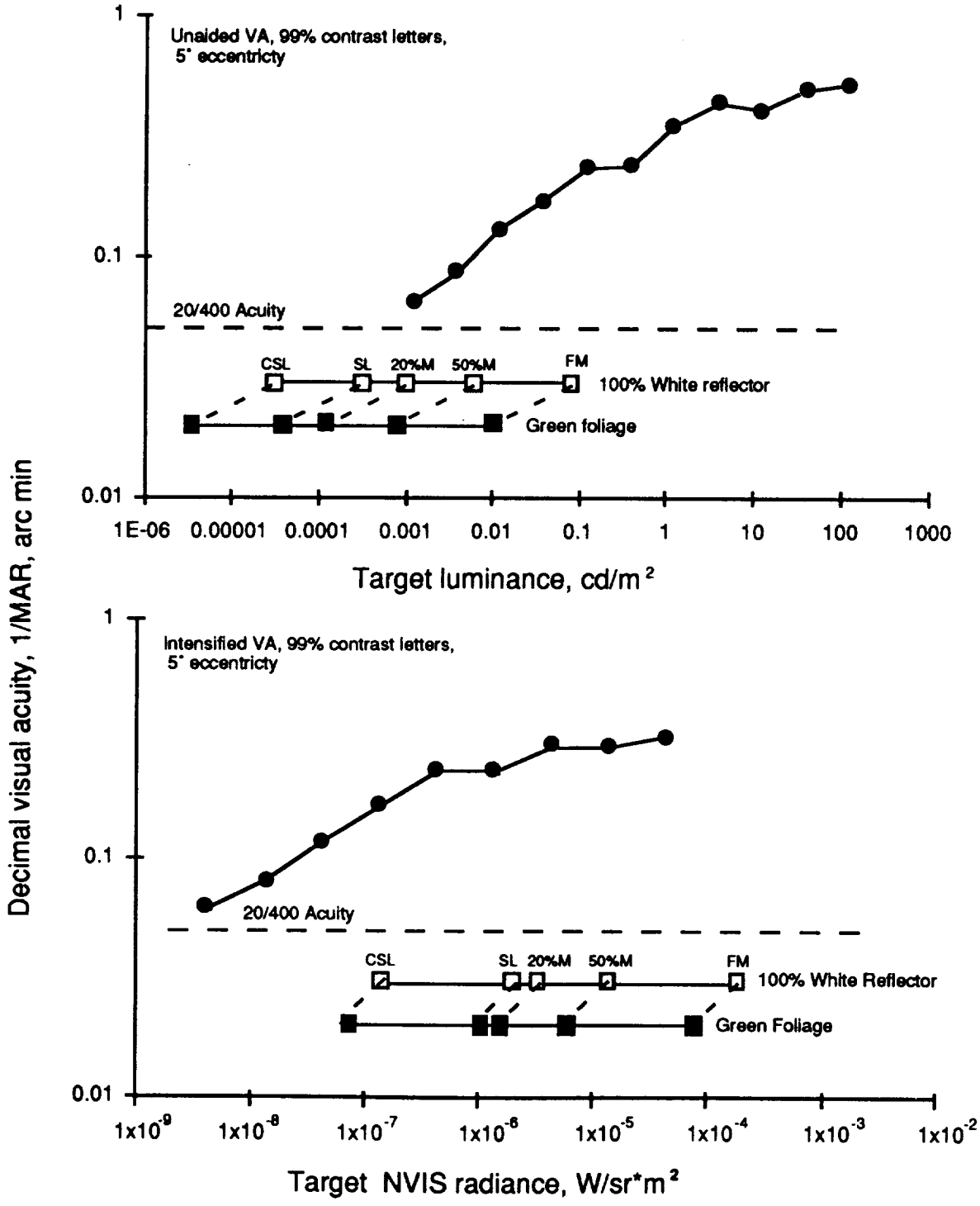

Figure 21. The relationship between the lighting levels used in the laboratory experiment and those experienced in the nocturnal environment are shown.

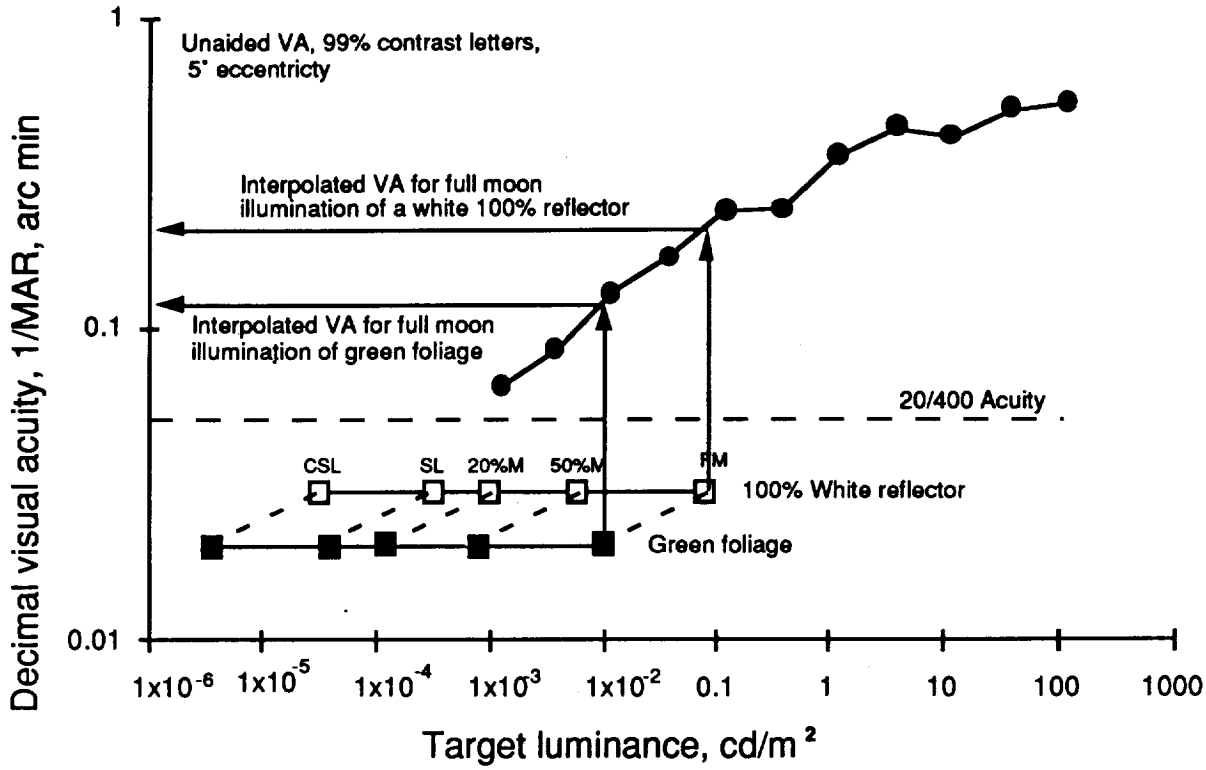

Figure 22. The method for interpolating visual acuity expected under a variety of environmental conditions.

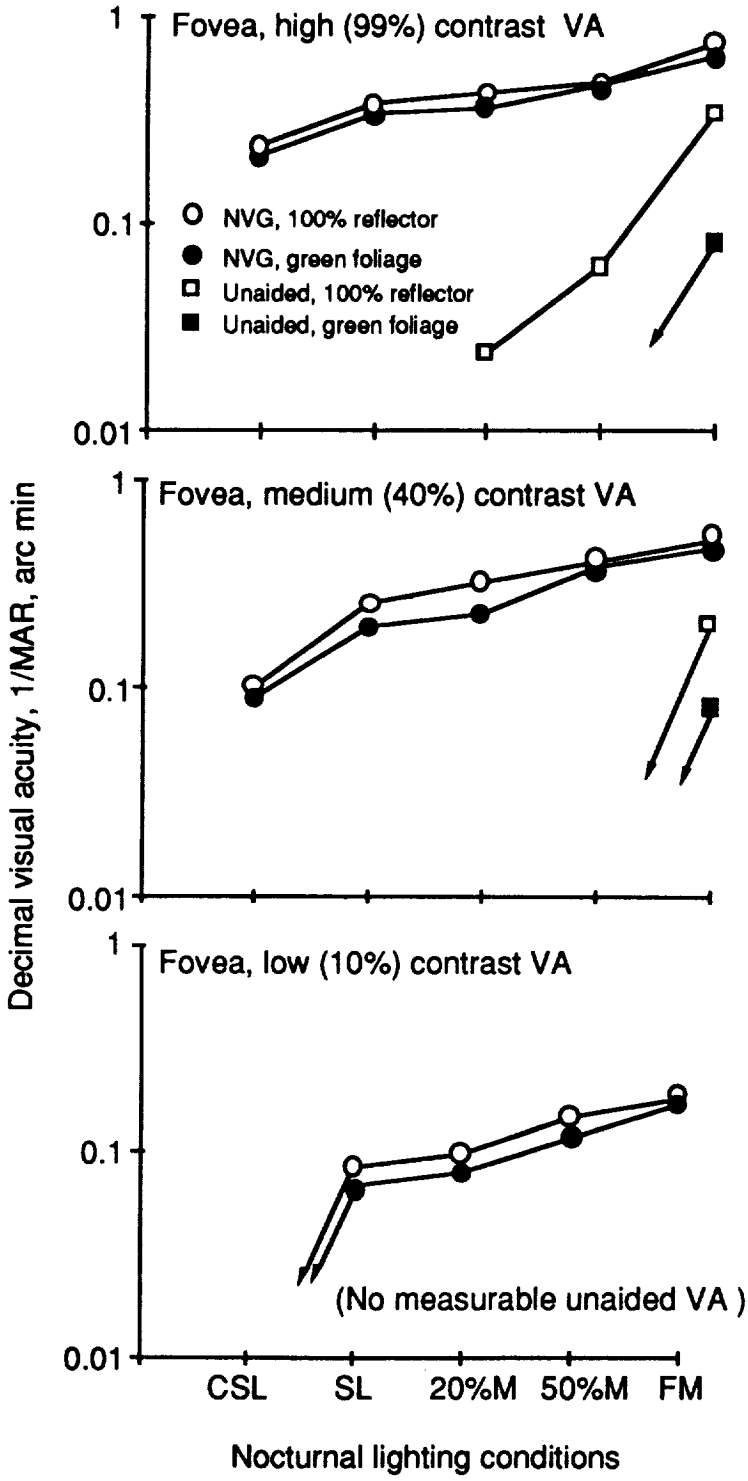

Figure 23. VA for aided (circles) and unaided (squares), for two reflectors (open = white paper, filled = green foliage) and for three different target contrasts: foveal.

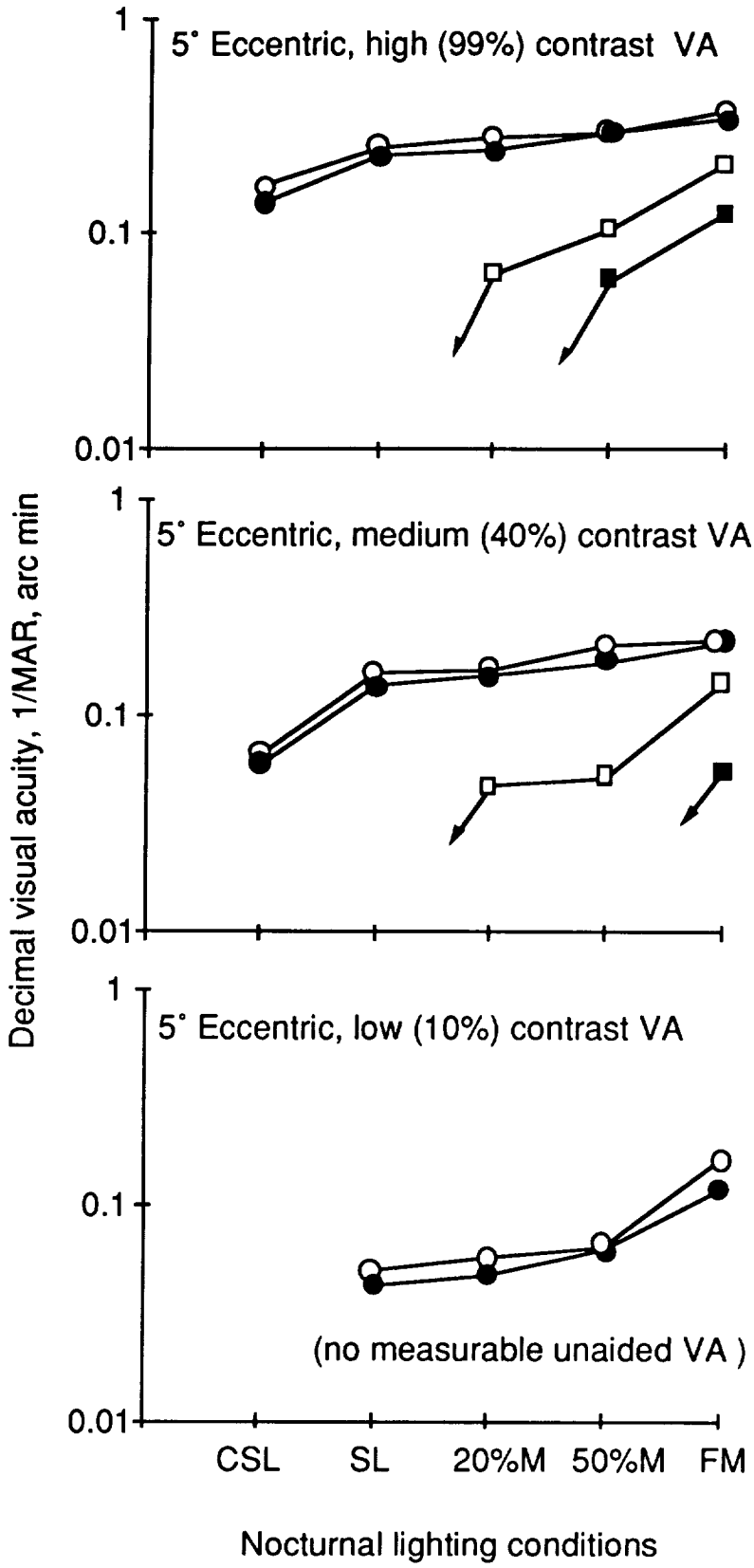

Figure 24. Same as figure 23 except for 5° eccentric.

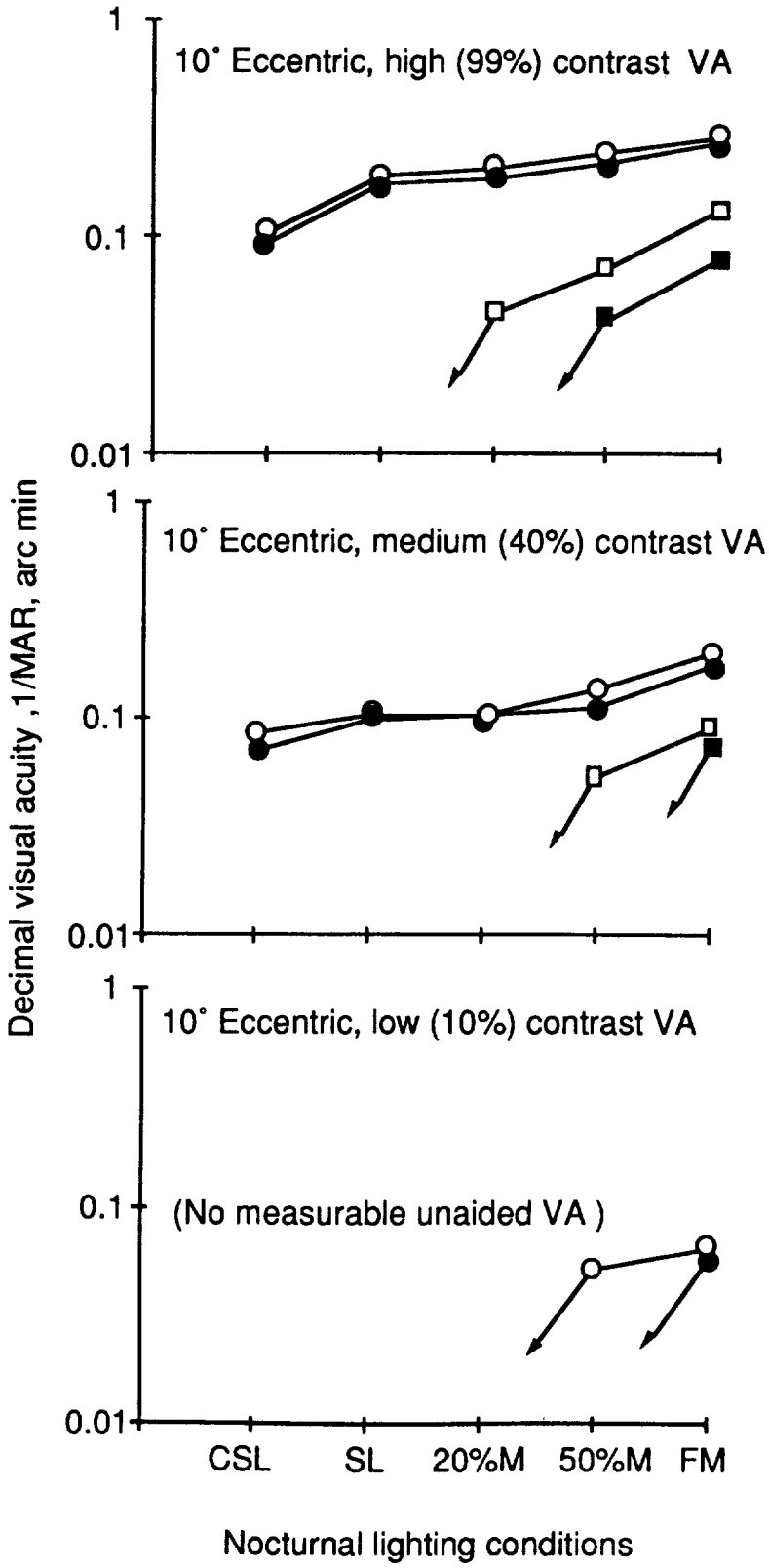

Figure 25. Same as figure 23 except for 10° eccentric.

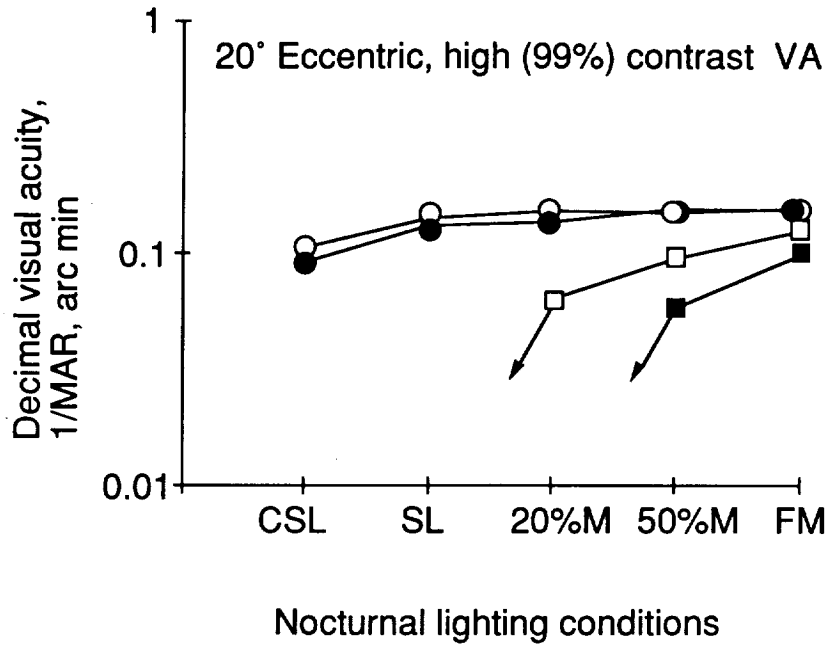

Figure 26. Same as figure 23 except for 20° eccentric and for high (99%) target contrast only.

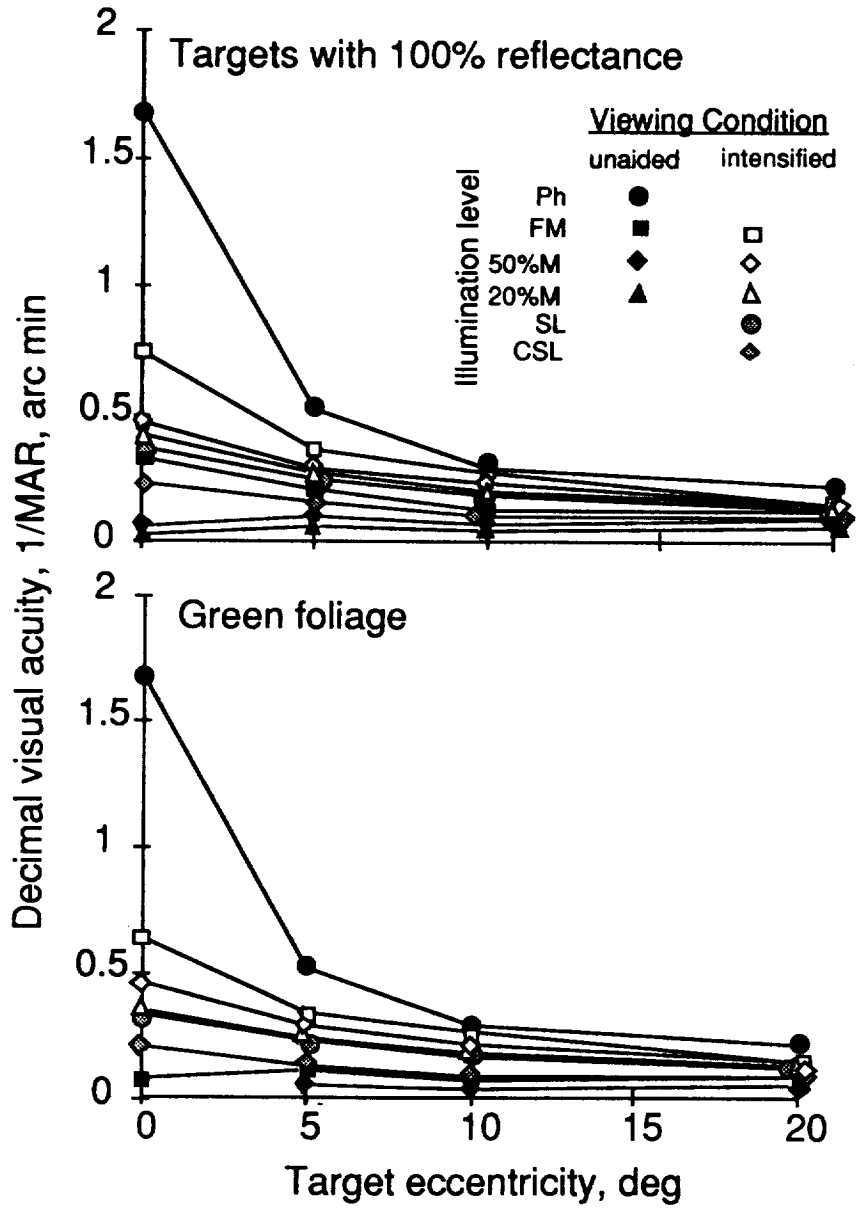

Figure 27. Visual acuity on a linear scale as function of target eccentricity for range of environmental conditions.

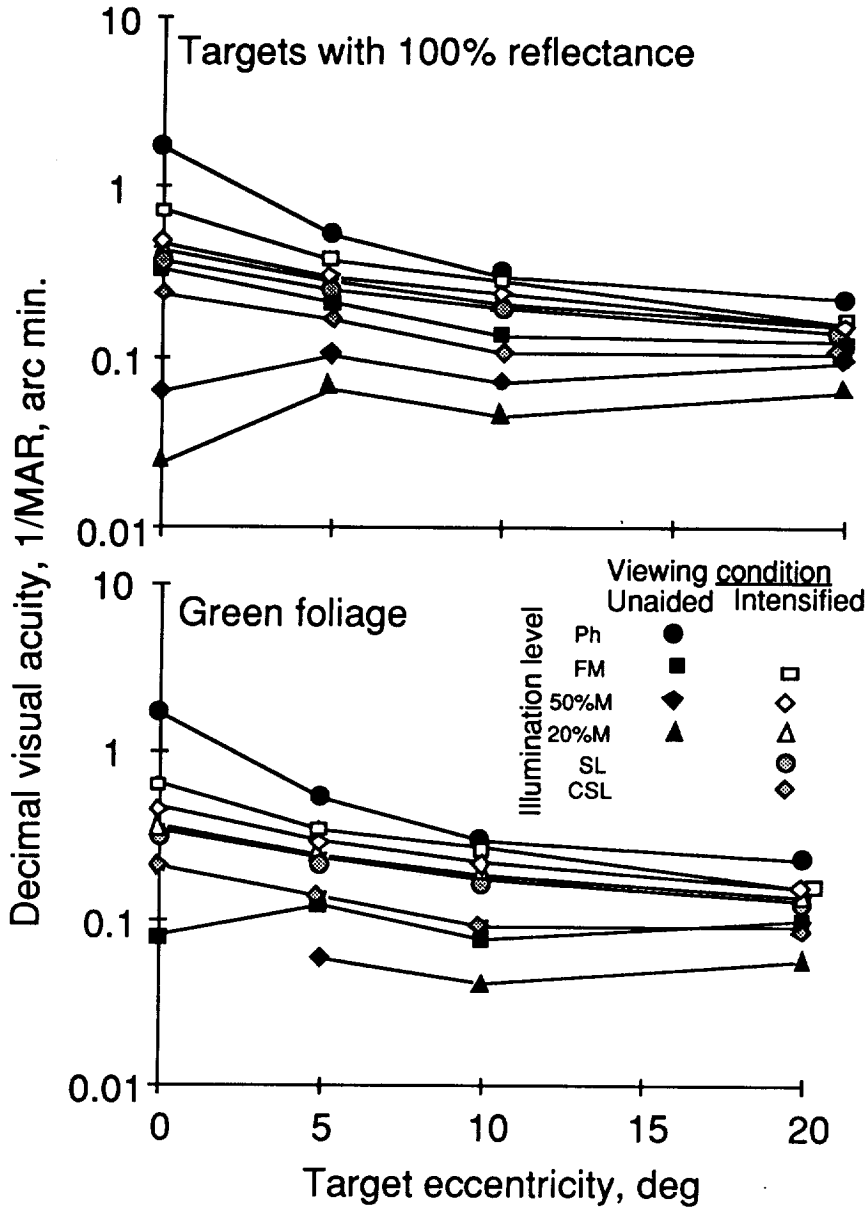

Figure 28. Visual acuity on a log scale as function of target eccentricity for a range of environmental conditions.

REPORT DOCUMENTATION PAGE

Form Approved
OMB No. 0704-0188

1. AGENCY USE ONLY *(Leave blank)*	2. REPORT DATE	3. REPORT TYPE AND DATES COVERED
	January 1994	Technical Memorandum

4. TITLE AND SUBTITLE

Evaluation of Visual Acuity with Gen III Night Vision Goggles

5. FUNDING NUMBERS

505-6436

6. AUTHOR(S)

Arthur Bradley* and Mary K. Kaiser

7. PERFORMING ORGANIZATION NAME(S) AND ADDRESS(ES)

Ames Research Center
Moffett Field, CA 94035-1000

8. PERFORMING ORGANIZATION REPORT NUMBER

A-93134

9. SPONSORING/MONITORING AGENCY NAME(S) AND ADDRESS(ES)

National Aeronautics and Space Administration
Washington, DC 20546-0001

10. SPONSORING/MONITORING AGENCY REPORT NUMBER

NASA TM-108792

11. SUPPLEMENTARY NOTES

Point of Contact: Mary K. Kaiser, Ames Research Center, MS 262-3, Moffett Field, CA 94035-1000; (415) 604-4448
*Indiana University, School of Optometry, Indiana

12a. DISTRIBUTION/AVAILABILITY STATEMENT

Unclassified — Unlimited
Subject Category 54

12b. DISTRIBUTION CODE

13. ABSTRACT ***(Maximum 200 words)***

Using laboratory simulations, visual performance was measured at luminance and night vision imaging system (NVIS) radiance levels typically encountered in the natural nocturnal environment. Comparisons were made between visual performance with unaided vision and that observed with subjects using image intensification. An Amplified Night Vision Imaging System (ANVIS6) binocular image intensifier, manufactured by ITT (employing their Gen III tube), was used. Light levels available in the experiments (using video display technology and filters) were matched to those of reflecting objects illuminated by representative night-sky conditions (e.g., full moon, starlight). Results show that as expected, the precipitous decline in foveal acuity experienced with decreasing mesopic luminance levels is effectively shifted to much lower light levels by use of an image intensification system. The benefits of intensification are most pronounced foveally, but still observable at 20° eccentricity. Binocularity provides a small improvement in visual acuity under both intensified and unintensified conditions.

14. SUBJECT TERMS	15. NUMBER OF PAGES
Visual acuity, Night vision goggles, Visual performance	39
	16. PRICE CODE: A03

17. SECURITY CLASSIFICATION OF REPORT	18. SECURITY CLASSIFICATION OF THIS PAGE	19. SECURITY CLASSIFICATION OF ABSTRACT	20. LIMITATION OF ABSTRACT
Unclassified	Unclassified		